

27, 765 (1971).

²⁴R. P. Feynman, in *High Energy Collisions*, Third International Conference held at State University of New York, Stony Brook, 1969, edited by C. N. Yang, J. A. Cole, M. Good, R. Hwa, and J. Lee-Franzini (Gordon and Breach, New York, 1969).

²⁵The question of the ultimate fate of the fractional charge may be a difficulty of the quark-parton model. B. Ioffe [Phys. Letters 30B, 123 (1960)] estimates z , the important longitudinal distances in configuration space for electroproduction, to be of the order $M_p^{-1} \omega$, where ω is the usual scaling variable. This may imply that the active parton tends to travel a considerable distance without interaction before disintegrating into a jet of hadrons. Thus, there can be a separation of fractional charge over large distances in configuration space as well as momentum space. However, this does not mean that partons must "backflow" that distance to provide the necessary neutralization of fractional charge.

This can be accomplished, for example, by a polarization current created by parton-antiparton pairs created from the vacuum by the field of the active parton. This is also related to a problem raised by R. Dashen [cf. M. Gell-Mann, invited talk at the International Conference on Duality and Symmetry in Hadron Physics, Tel Aviv, 1971 (unpublished)].

²⁶For example, see N. Bali, Lowell Brown, R. Peccei, and A. Pignotti, Ref. 4.

²⁷L. Caneschi, C. H. Mehta, and H. J. Yesian, Stanford University Report No. ITP 380, 1971 (unpublished).

²⁸This happens, for example, with the CKP distribution (cf. G. Cocconi, L. Koester, and D. Perkins, Ref. 4).

²⁹J. D. Bjorken, invited talk at the International Conference on Duality and Symmetry in Hadron Physics, Tel Aviv, 1971 (unpublished). This particular quark-parton model has also been discussed and used in several calculations by J. Kuti and V. Weisskopf, this issue, Phys. Rev. D 4, 3418 (1971).

PHYSICAL REVIEW D

VOLUME 4, NUMBER 11

1 DECEMBER 1971

Inelastic Lepton-Nucleon Scattering and Lepton Pair Production in the Relativistic Quark-Parton Model*

Julius Kuti† and Victor F. Weisskopf

*Laboratory for Nuclear Science and Department of Physics, Massachusetts Institute of Technology,
Cambridge, Massachusetts 02139*

(Received 26 July 1971)

We discuss the interaction of hadrons with leptons in the limit of large momentum transfer. A special parton model will be used for the hadrons in which the partons are identified with quarks. The relativistic quark model with which we interpret recent observations is formulated as follows: (1) The baryons are composed of three valence quarks and a core of an indefinite number of quark-antiquark pairs. (2) The lepton "sees" the nucleon in the limit of large momenta in the c.m. frame as an assembly of freely moving constituents with point charges. (3) The scattering of the valence quarks is interpreted as the nondiffractive component, the scattering of the core is interpreted as the diffractive component of the cross section. (4) The nondiffractive scattering is assumed to be mediated by suitable meson exchanges, and this assumption determines the momentum distribution of the valence quarks. The $(q\bar{q})$ pairs in the core are assumed to be distributed statistically in the available phase space. (5) It will be necessary to include "gluons" among the constituents of the nucleon. They are supposed to be the uncharged quanta of the force field between quarks and are assumed to be distributed statistically over the momentum space. There is only one constant adjustable in this model, which is the ratio of gluons to core pairs. All other constants are fixed by simple considerations. This model is used to calculate the deep-inelastic scattering of electrons by protons and neutrons and its dependence on the relative spin orientations, the inelastic scattering of neutrinos by nucleons, and the creation of massive muon pairs by proton-proton collisions. After adjusting the open constant to the data of electron-proton scattering, the theory predicts unambiguously the other results. They are in reasonably good agreement with the observations as far as they are known.

I. INTRODUCTION

The ideas presented here are inspired by efforts of many authors who have faced the challenge: What is the nucleon made of? Much in this paper has a considerable overlap with the work of others in the field, and we have included some well-known

ideas in the interest of clarity and completeness.

In studying the substructure of a hadron, one must keep in mind an essential difference between hadrons and systems such as the nuclei or atoms. In the latter cases the relevant energies – binding energies, excitation energies, etc. – are much smaller than the rest masses of the system as a

whole or of the constituents; in the case of hadrons, however, they are of the same order as the mass of the system; obviously the mass of the constituents is not known. This difference is a fundamental one; it puts the use of the concept "constituent" into question. In the nuclear and atomic systems the number and nature of the constituents is well defined, particle-antiparticle pairs play a subordinate role such as in the effect of the polarization of the vacuum. In hadrons, however, there is no well-defined number of constituents, since the interaction energies are so strong that virtual pairs of fermions or virtual single bosons are abundantly present. This is certainly true of mesons which make up the "meson cloud" of the nucleon. The description of the nucleon, therefore, cannot be formulated in terms of a fixed number of constituents.

Nevertheless, in hadron phenomena a number of remarkably simple properties have been realized in the past few years. Beyond the well-known agreements with relativity, analyticity, unitarity, etc. there are the conservation rules of isospin and strangeness and an approximate agreement with SU(3) symmetry. In addition to these concepts we realize other empirical regularities in extreme high-energy collisions which might lead us toward a dynamical understanding of the hadron structure.

We begin by listing a partial list of regularities which are more or less established experimentally, and which will be used in this paper as indications of hadron structure.

(1) SU(3) is an approximate symmetry in nature. Baryons and mesons belong to SU(3) multiplets; strong-interaction cross sections and current matrix elements in electromagnetic and weak interactions yield further evidence for this symmetry scheme. No exotic hadrons seem to exist. The hadron spectrum is similar to the orbital and radial excitations of oscillator-like bound quark structures.

(2) The total cross sections become diffractive at high energies, the object exchanged in the t channel to explain the diffractive behavior has vacuum quantum numbers.

(3) Exchange-reaction cross sections fall with a power of the energy $s^{2\alpha-2}$. This empirical fact will be used to determine the momentum distribution of valence quarks, assumed to be associated with the nondiffractive mechanism of the scattering process.

(4) Cross sections fall rapidly with transverse momentum transfer. The average transverse momentum of the particles in inelastic collisions is limited (to about 0.35 GeV/c). This fact is relevant in learning about the transverse momentum distri-

bution of constituents inside the nucleon.

Feynman¹ suggested that many of the observed regularities might fit an underlying parton picture. We identify the partons with the Zweig-Gell-Mann quarks. Certain observations under (1) have made this picture attractive. It is the purpose of the paper to show that the quark model has some degree of organizing and predictive power when applied to deep-inelastic electron-nucleon scattering, to neutrino induced reactions, and to $\mu^+\mu^-$ production in proton-proton collisions.

A truly relativistic quantum-mechanical theory, appropriate to deal with both short-distance behavior of current matrix elements and with pure hadronic reactions, seems today available only in field theory. Its mathematical description is so complex that no dynamical regularities can be expected, other than those following from symmetries and lucky guesses about extreme asymptotic limits. We choose to make use of the parton model, sacrificing detailed theoretical adequacy for simplicity.

Bjorken, Drell, Feynman, and their collaborators have in the past discussed simple parton models in the impulse approximation.¹⁻³ They have shown that the main qualitative features of the data seem to be reproduced in that extreme asymptotic limit.

To apply the impulse approximation, we analyze the bound system - be it a nucleon, nucleus, or atom - in terms of its constituents, called partons. Nucleons and electrons are the partons of the nucleus and atom whereas in our model the partons of the nucleon are quarks. If the kinematics is such that the partons can be treated as instantaneously free during the sudden pulse carrying a large energy transfer from the projectile, we can then hope to neglect their binding effects during the interaction. We conjecture that in deep-inelastic electron scattering the virtual photon takes a snapshot of the instantaneous nucleon substructure when the momentum transfer $|q|$ of the virtual quantum is large compared to the momentum transfers between partons in the internal motions. We assumed the latter to be of the order $\sim M$. Hence, the condition for the validity of the impulse approximation is $|q| \gg M$.

In that way, for reactions involving massive currents, we choose a relativistic theory which is naive and inadequate in its simplicity, but one which is definite and in which we can calculate many processes in order to see how closely our approximation in the extreme asymptotic limit gives a partial reflection of reality.

The paper is organized as follows. In Sec. II we formulate the specific details of the relativistic

quark model, which we propose to be probed in the impulse approximation. In Sec. III we analyze the high-energy inelastic electron-nucleon scattering experiments within the framework of the parton model. Section IV presents a test of the quark-parton model, the spin dependence of inelastic electron- (muon-) proton scattering. In Sec. V we calculate the massive $\mu^+ \mu^-$ pair production in nucleon-nucleon collisions. In Sec. VI we discuss some implications of the model in high-energy inelastic neutrino-nucleon scattering. The detailed analysis of this process will be published elsewhere. Finally, concluding remarks comprise Sec. VII. Here we list some well-known difficulties such as the absence of free quarks. The expectation to "see" them as free particles may be based on our unlimited extrapolation of present-day laws to those enigmatic objects.

In Appendix A we rederive the well-known expressions for the inelastic structure functions in the c.m. electron-proton coordinate system in terms of the single-particle momentum distributions. The derivation of the spin-dependent structure functions is new here. Appendix B contains the calculation of the parton momentum distributions on the basis that the probability distribution of core quarks is proportional to the relativistic phase space, and the distribution of the valence quarks is given by a Regge-pole consideration. Appendix C contains arguments for the presence of uncharged gluons in the nucleon. Appendix D contains a discussion of the behavior of the structure functions at threshold and the relation of this behavior to the elastic form factor.

II. THE QUARK MODEL AND ITS IMPULSE APPROXIMATION

We consider the nucleon to be a three-quark structure accompanied by a core of virtual quark-antiquark pairs:

$$N \rightarrow qq\bar{q} + \eta(q\bar{q}).$$

The valence quarks carry the internal quantum numbers of the nucleon, whereas the core has vacuum numbers. The number η of virtual $q\bar{q}$ pairs depends on the frame of reference. We assume that the masses, binding energies, and internal momenta of the quarks (in the rest frame) are of the order M (proton mass) or less. This assumption is suggested (but not proven) by the experimental fact that the lateral momenta of collision products are small, which may point towards small internal momenta among the constituents. Under these assumptions, a nucleon moving with a momentum $P \gg M$ could be considered as composed of n almost free particles, $\frac{1}{2}(n+3)$ quarks, and $\frac{1}{2}(n-3)$ antiquarks, all moving almost parallel in

the direction of P . The idealized picture of a nucleon as a parallel stream of free particles is called the impulse approximation and the deviations from this idealization can be neglected when interactions of large momentum transfer ($Q^2 \gg M^2$) are considered.

What can be said about the number η of particles and their momentum distribution?

(a) In the decomposition of the nuclear wave function the total three-momentum \vec{P} is conserved. In the longitudinal direction we get

$$\sum P_i = P \quad \text{or} \quad \sum x_i = 1, \quad x_i = P_i/P$$

where P_i is the longitudinal momentum of the i th parton. It is easy to see that P_i must be positive if it is much larger than M . In this case the parton moves essentially with light velocity and its energy $\epsilon_i \sim |P_i|$, since both its mass and its transverse momentum is of the order M or smaller. If all P_i are positive, the sum of all the energies will be about equal to the energy P of the proton, to the order M^2/P . If one P_i or more are negative, $\sum(\epsilon_i - P_i) > M$; such a state would be much further from the mass shell than those with all P_i positive and therefore will be highly improbable.

(b) In dealing with $q\bar{q}$ pairs in the core, we have to describe a system with an infinite number of degrees of freedom. Statistical considerations are suggestive here; therefore, as a first try we assume that the probability distribution of quarks in the core is proportional to the phase space,

$$dP_c(x) \sim g \frac{dx}{(x^2 + \mu^2/P^2)^{1/2}}, \quad (2.1)$$

where $\mu \sim M$ is the effective mass of the quarks. As (2.1) shows, the calculation in this paper will be carried out with a sharp δ -function cutoff [$f(k_i) \sim \delta(k_i)$] in the transverse momenta k_i , although the essential features of the model remain unchanged introducing a smooth cutoff function $f(k_i)$ in the probability distribution.

Qualitative arguments might indicate that g is of order unity. The spectrum for core quarks in (2.1) implies that their total number is logarithmically increasing as $\ln(P/\mu)$. If core quarks are somehow converted into real particles in the collision process, then $g \sim 1$ is suggested from the observed logarithmic energy dependence of pion multiplicity in high-energy collisions.

The longitudinal momentum distribution (2.1) is strongly reminiscent of the apparent photon distribution in the field of a fast-moving electric charge according to the Weizsäcker-Williams method. The constant g is then replaced by a constant of the order $e^2/\hbar c$. The analogy with the Weizsäcker-Williams method is instructive for the understanding of the virtual nature of the $q\bar{q}$ pairs. The num-

ber of these pairs is not invariant, in the same sense as the number of photons accompanying the moving charge is not invariant. It is the number of virtual pairs or photons which are near enough to the mass shell to be treated as quasi-free. This is why the following two statements are not contradictory: (1) There are very few partons with momenta much larger than M in a nucleon at rest; (2) The most probable momentum of a parton in a fast-moving nucleon is a small momentum ($\sim M$).

(c) The longitudinal momentum distribution of valence quarks is given by

$$dP_v(x) \sim \frac{\psi(x)}{(x^2 + \mu^2/P^2)^{1/2}} dx, \quad (2.2)$$

where $\psi(x)$ depends on the special dynamics of the valence quarks. They are not assumed to be distributed statistically. We will show later that $\psi(x) \sim x^{1-\alpha(0)}$ follows from an application of Regge theory. Here $\alpha(0) \sim \frac{1}{2}$ is the intercept of the important nondiffractive trajectories in inelastic lepton-nucleon scattering. A_2, P' are exchanged in inelastic electron-nucleon scattering, whereas vector trajectories contribute to the neutrino-induced reactions. A common $\alpha(0) \sim \frac{1}{2}$ will do the job for both types of processes.

It is true that $\psi(x) \sim x^{1-\alpha(0)}$ is dictated by Regge lore only for x near zero, in the asymptotic region. (In Sec. III we will show that $x \rightarrow 0$ for fixed virtual photon mass corresponds to $W^2 \rightarrow \infty$, where W is the invariant mass of hadrons created in the virtual photoabsorption process.) We kept the form $\psi(x) \sim x^{1-\alpha(0)}$ in the whole $(0, 1)$ interval for the sake of simplicity. Evidently, any sophistication in $\psi(x)$ might lead to better results. Ignoring complexities in the valence structure is not unreasonable if we want to keep all of the model assumptions on the same level of simplicity.

On the basis of these assumptions the probability distribution of an n -quark state is

$$dP_n(x_1 \cdots x_n) = Z \frac{g^k}{k!} \delta\left(1 - \sum_{j=1}^n x_j\right) \times \prod_{i=1}^3 x_i^{1-\alpha(0)} \prod_{j=1}^n \frac{dx_j}{(x_j^2 + \mu^2/P^2)^{1/2}}, \quad (2.3)$$

where Z is an over-all normalization constant, $n = 3 + k$ ($k = 0, 2, 4, \dots$ counts the quarks and antiquarks in the core). Z is not a free parameter in the model since the total probability has to be normalized to unity. The factor $g^k/k!$ in Eq. (2.3) is the statistical weight appropriate to symmetric particles, as suggested by the analysis of the SU(3) multiplets.

There is one modification that we have included in the actual calculation (Appendix B). To distinguish the three different quarks ($\phi, \mathfrak{N}, \lambda$) in the core, we replaced the simple factor $g^k/k!$ by

$$\frac{g^k}{k!} \rightarrow \frac{(\frac{1}{3}g)^{k_1} (\frac{1}{3}g)^{k_2} (\frac{1}{3}g)^{k_3}}{k_1! k_2! k_3!}, \quad (2.4)$$

with $k = k_1 + k_2 + k_3$, where k_1, k_2 , and k_3 are even positive numbers. We still do not distinguish quarks from antiquarks for simplicity reasons only. The replacement (2.4) does not bring any change in the final result.

We have not discussed the mediator of interaction between quarks. Nothing is known about that. If we want to manifest the interaction in terms of field quanta, then neutral mesons (gluons) are the obvious candidates. Indeed, there are indications from the MIT-SLAC experiments⁴ that the average squared charge per constituent is less than expected in a quark model without neutral quanta (see Appendix C). It is plausible to assume that the momentum distribution of the gluons is the same as for core quarks, apart from replacing the constant g by g' : To include gluons, we replace Eq. (2.3) by

$$dP_n(x_1 \cdots x_n) = Z \frac{(\frac{1}{3}g)^{k_1} (\frac{1}{3}g)^{k_2} (\frac{1}{3}g)^{k_3} g'^l}{k_1! k_2! k_3! l!} \delta\left(1 - \sum_{j=1}^n x_j\right) \times \prod_{i=1}^3 x_i^{1-\alpha(0)} \prod_{j=1}^n \frac{dx_j}{(x_j^2 + \mu^2/P^2)^{1/2}}, \quad (2.5)$$

with $n = 3 + k_1 + k_2 + k_3 + l$, where $l = 0, 1, 2, \dots$ is the number of gluons in the n -particle state.

The expression (2.5) can be used to determine the following probability functions, which are of importance in our discussions of actual processes: $G_i^{p,n}(x) dx$, $i = 0, 1, 2, 3$ is defined as the probability in a proton (p) or a neutron (n) with momentum $P \gg M$ to find a parton or its antiparticle of type i with a momentum between $P \cdot x$ and $P \cdot (x + dx)$. The labels $i = 1, 2, 3$ refer to quarks of the $\phi, \mathfrak{N}, \lambda$ type, while $i = 0$ refers to the gluon. The following relations follow from SU(3) considerations:

$$G_1^p(x) = G_2^n(x), \quad G_2^p(x) = G_1^n(x), \quad G_3^p(x) = G_3^n(x), \quad (2.6)$$

$$G_0^p(x) = G_0^n(x).$$

We divide these functions into two parts:

$$G_i^p(x) = G_{iv}^p(x) + G_{ic}^p(x),$$

where the first term refers to the valence quarks and the second to the core quarks. These functions are connected with (2.5) in the following way:

$$\begin{aligned}
G_{1v}^p(x) &= 2G_{2v}^p(x) = 2Z \frac{x^{1-\alpha(0)}}{(x^2 + \mu^2/P^2)^{1/2}} \sum_{k_i=0,2,\dots;l=0,1,2,\dots} \frac{(\frac{1}{3}g)^{k_1}(\frac{1}{3}g)^{k_2}(\frac{1}{3}g)^{k_3}g'^l}{k_1!k_2!k_3!l!} \\
&\quad \times \int \prod_{j=1}^{n-1} \frac{dx_j}{(x_j^2 + \mu^2/P^2)^{1/2}} x_1^{1-\alpha(0)} x_2^{1-\alpha(0)} \delta\left(1 - x - \sum_{j=1}^{n-1} x_j\right), \\
G_{3v}(x) &= G_{0v}(x) = 0, \\
G_{1c}^p(x) &= G_{2c}^p(x) = G_{3c}^p(x) = Z \frac{1}{(x^2 + \mu^2/P^2)^{1/2}} \sum_{k_i=0,2,\dots;l=0,1,2,\dots} k_1 \frac{(\frac{1}{3}g)^{k_1}(\frac{1}{3}g)^{k_2}(\frac{1}{3}g)^{k_3}g'^l}{k_1!k_2!k_3!l!} \\
&\quad \times \int \prod_{j=1}^{n-1} \frac{dx_j}{(x_j^2 + \mu^2/P^2)^{1/2}} x_1^{1-\alpha(0)} x_2^{1-\alpha(0)} x_3^{1-\alpha(0)} \delta\left(1 - x - \sum_{j=1}^{n-1} x_j\right), \\
G_{0c}^p(x) &= 3 \frac{g'}{g} G_{1c}^p(x).
\end{aligned} \tag{2.7}$$

The integrals and summations are carried out in Appendix B and yield for $x > \mu/P$

$$\begin{aligned}
G_{1v}^p &= 2G_{2v}^p = 2 \frac{\Gamma(\gamma + 3[1 - \alpha(0)])}{\Gamma(1 - \alpha(0))\Gamma(\gamma + 2[1 - \alpha(0)])} x^{-\alpha(0)}(1-x)^{-1+\gamma+2[1-\alpha(0)]}, \\
G_{1c}^p &= G_{2c}^p = G_{3c}^p = \frac{g}{3g'} G_{0c}^p(x) = \frac{1}{3}g x^{-1+\gamma+3[1-\alpha(0)]},
\end{aligned} \tag{2.8}$$

with $\gamma = g + g'$. Obviously we have

$$\frac{1}{2} \int G_{1v}^p(x) dx = \int G_{2v}^p(x) dx = 1. \tag{2.9}$$

The only undetermined constants are g and g' . $\alpha(0)$ is determined by Regge considerations as will be shown later.

In the limit $x \rightarrow 0$ the core contributions are dominant,

$$G_i(x) = G_{ic}(x) = \frac{\text{const}}{x} \quad \text{for } x \rightarrow 0. \tag{2.10}$$

In the limit $x \rightarrow 1$ the valence contributions are dominant for $i = 1, 2$,

$$\begin{aligned}
G_1(x) &= G_{1v}(x) = 2 \frac{\Gamma(\gamma + 3(1 - \alpha))}{\Gamma(1 - \alpha)\Gamma(\gamma + 2(1 - \alpha))} (1-x)^{-1+\gamma+2(1-\alpha)}, \\
G_2(x) &= G_{2v}(x) = \frac{1}{2} G_{1v}(x) \quad \text{for } x \rightarrow 1.
\end{aligned} \tag{2.11}$$

III. DEEP-INELASTIC ELECTRON-NUCLEON SCATTERING

A. Kinematics

The kinematics of the spin-averaged process is well known. We recite the most important kinematic relations to keep the paper self-contained. The cross section for a proton (of mass M) with momentum P_μ to scatter a high-energy electron (of mass m) from initial momentum $k_{1\mu}$ to final momentum $k_{2\mu}$ in the range d^3k_2 can be written as follows:

$$d\sigma = \frac{\alpha^2}{4\pi} q^{-4} [(k_1 \cdot P)^2 - m^2 M^2]^{-1/2} L_{\mu\nu} W^{\mu\nu} \frac{d^3k_2}{E_2}. \tag{3.1}$$

In Eq. (3.1) an average over the initial electron and proton spin is understood; also we sum over hadrons and the electron spin in the final state. The

virtual photon transmitted has four-momentum q_μ . $L_{\mu\nu}$ is defined as the contribution of the electron-photon vertex,

$$L_{\mu\nu} = 2(k_{1\mu}k_{2\nu} + k_{2\mu}k_{1\nu} - k_1 \cdot k_2 g_{\mu\nu} + m^2 g_{\mu\nu}), \tag{3.2}$$

whereas the hadronic current amplitude $W_{\mu\nu}(P, q)$ can be expressed in terms of the two famous structure functions $W_1(q^2, \nu)$ and $W_2(q^2, \nu)$:

$$\begin{aligned}
W_{\mu\nu}(P, q) &= 4\pi M \left(\frac{q_\mu q_\nu}{q^2} - g_{\mu\nu} \right) W_1(q^2, \nu) \\
&\quad + \frac{4\pi}{M} \left(P_\mu - \frac{P \cdot q}{q^2} q_\mu \right) \left(P_\nu - \frac{P \cdot q}{q^2} q_\nu \right) W_2(q^2, \nu).
\end{aligned} \tag{3.3}$$

$W_{\mu\nu}(P, q)$ is the commutator function of the electromagnetic current for spacelike q_μ ,

$$W_{\mu\nu}(P, q) = \frac{1}{2} \sum_{\xi} \int d^4x e^{i q x} \langle P, \xi | [j_{\mu}(x), j_{\nu}(0)] | P, \xi \rangle, \quad (3.4)$$

where ξ_{μ} denotes the covariant spin of the proton. Equation (3.4) has triggered a great deal of work dedicated to the light-cone behavior of current commutators.

Next, we give the cross-section formula in the rest frame of the proton (where the electron scattering angle is θ):

$$\frac{d^2\sigma}{d\Omega dE_2} = \frac{d\sigma_{\text{Mott}}}{d\Omega} [W_2(q^2, \nu) + 2 \tan^2(\frac{1}{2}\theta) W_1(q^2, \nu)], \quad (3.5)$$

with

$$\frac{d\sigma_{\text{Mott}}}{d\Omega} = \frac{\alpha^2 \cos^2(\frac{1}{2}\theta)}{4E_1^2 \sin^4(\frac{1}{2}\theta)},$$

$$q^2 = q_0^2 - \vec{q}^2,$$

$$-Q^2 = q^2 = -4E_1 E_2 \sin^2(\frac{1}{2}\theta) \text{ in the lab system,}$$

and ν being the energy loss of the electron in the lab system, $\nu = M^{-1} P \cdot q$.

In Eq. (3.5) the mass of the high-energy electron is neglected. Hand expresses the cross section in terms of total absorption cross sections for transverse and scalar virtual photons,

$$\frac{d^2\sigma}{d\Omega dE_2} = \Gamma(\sigma_T + \epsilon\sigma_S), \quad (3.6)$$

where

$$\sigma_T = \frac{4\pi^2\alpha}{K} W_T, \quad (3.7)$$

$$\sigma_S = \frac{4\pi^2\alpha}{K} W_L,$$

with

$$W_T = W_1, \quad (3.8)$$

$$W_L = W_2(1 - \nu^2/q^2) - W_1.$$

Γ is the flux of virtual photons and K their effective momentum,

$$\Gamma = \frac{\alpha}{4\pi^2} \frac{2E_2 K}{E_1 q^2 (\epsilon - 1)}, \quad (3.9)$$

$$K = \frac{W^2 - M^2}{2M}, \quad W^2 = (P + q)^2.$$

The quantity ϵ lies in the range 0 to 1 and is the longitudinal-transverse polarization ratio of the source of virtual photons provided by the scattering electron,

$$\epsilon = \frac{1}{1 + 2 \tan^2(\frac{1}{2}\theta)(1 - \nu^2/q^2)}. \quad (3.10)$$

The quantity R , often cited in both experimental and theoretical papers, is defined as the ratio of the probability for longitudinal photon absorption to that for transverse photons,

$$R = \frac{W_L(q^2, \nu)}{W_T(q^2, \nu)}. \quad (3.11)$$

B. Results from the Relativistic Quark Model

Now we are ready to calculate the structure functions $W_1(q^2, \nu)$ and $W_2(q^2, \nu)$ in the relativistic quark model in the impulse approximation.

For fixed and large q^2 and ν , the electron scattering angle $\theta_{\text{c.m.}}$ in the center-of-mass frame is small,

$$\theta_{\text{c.m.}} \sim Q/P, \quad (3.12)$$

in the $P \rightarrow \infty$ limit, so we can work close to the forward direction. According to the parton hypothesis, the proton in the c.m. frame is an assembly of fast-moving constituents with given momentum distributions. Suppose the quark "i" with charge e_i in electron units has a three-momentum $\vec{P}_i = x_i \vec{P}$; then it scatters the electron into the angle $\theta_{\text{c.m.}}$ with a cross section

$$\frac{d^2\sigma_i}{dQ^2 d\nu} = e_i^2 \frac{d\sigma_{\text{Mott}}}{dQ^2} \frac{x_i}{\nu} \delta(x - x_i), \quad (3.13)$$

where $x = Q^2/2M\nu$ is the invariant scaling variable in the scattering process. In Eq. (3.13) we introduced the covariant pointlike cross section

$$\frac{d\sigma_{\text{Mott}}}{dQ^2} = \frac{4\pi\alpha^2}{Q^4}. \quad (3.14)$$

The δ function ensures that the fraction x_i which determines the quark momentum is identical with the value of the scaling variable $x = Q^2/2M\nu$ whenever a quark scatters an electron.

The inelastic cross section of a nucleon can be derived from (3.13) by integrating over the probability distributions of the quark momenta,

$$\frac{d^2\sigma^{p,n}}{dQ^2 d\nu} = \frac{d\sigma_{\text{Mott}}}{dQ^2} \sum_{i=1}^3 e_i^2 \frac{x}{\nu} G_i^{p,n}(x). \quad (3.15)$$

Obviously we have $e_1^2 = \frac{4}{9}$ and $e_2^2 = e_3^2 = \frac{1}{9}$.

In the form (3.5) only the first term survives the limit $P \rightarrow \infty$, $\theta_{\text{c.m.}} \rightarrow 0$, and by comparison with (3.15) we get the scaling result,

$$\nu W_{2p,n}(q^2, \nu) = x \sum_{i=1}^3 e_i^2 G_i^{p,n}(x) \equiv F_{p,n}(x), \quad (3.16)$$

where x is the scaling variable. The fact that νW_2 is a function of only x is intimately connected with the pointlike structure of the partons. Indeed, the experiments have shown that, for fixed W , the cross section varies at high energies as q^{-4} , indi-

cating pointlike structures inside the nucleon. This is in full analogy to Rutherford's experiment which found a q^{-4} dependence in the high-energy scattering of α particles in atoms. The scaling of $\nu W_2(q^2, \nu)$ does not prove the existence of pointlike constituents, but pointlike constituents necessarily lead to scaling.

We now write

$$F_{p,n}(x) = F_{p,n}^v(x) + F^c(x),$$

where $F_{p,n}^v$ contains the contributions of the valence quarks and F^c those of the core quarks which are the same for p and n . With help of expressions (2.8) we get

$$F_p^v(x) = \frac{3}{2} F_n^v(x) = \frac{\Gamma(\gamma + 3(1 - \alpha))}{\Gamma(1 - \alpha)\Gamma(\gamma + 2(1 - \alpha))} x^{1-\alpha}(1-x)^{-1+\gamma+2(1-\alpha)}, \quad (3.17)$$

$$F^c(x) = \frac{2}{9} g(1-x)^{-1+\gamma+3(1-\alpha)}.$$

The asymptotic properties (2.10) of the G_i 's insure a finite value for $F_{p,n}$ in the limit of $x \rightarrow 0$, in agreement with experiments. In addition, we find $F_p(0) = F_n(0)$. For $x=1$, the valence quarks only contribute, and we see from (2.11) that

$$F_n/F_p = \frac{2}{3} \text{ for } x \rightarrow 1. \quad (3.18)$$

(See *Note added in proof.*) The value $\frac{2}{3}$ is easily understood: The scattering intensity should be proportional to the squared charge of the scattering quarks. For $x \sim 1$, only the three valence quarks contribute; hence the ratio of the cross sections for the two nucleons ought to be equal to the ratio of the sum of the squared charges of the three quarks which make up the nucleon in the primitive quark picture.

The result (3.18) is characteristic of the quark model. Bloom and Gilman⁵ obtain a different result from duality considerations. In their case this ratio is equal to the ratio of the squares of the magnetic moments: $F_n/F_p \sim (\frac{2}{3})^2$. In quark-model language, their result is the ratio of the square of the geometrical sum of the quark magnetic moments, whereas our result is the ratio of the sum of the squares of the quark magnetic moments. In our case the quarks scatter incoherently even in the limit $x \rightarrow 1$; in their case the scattering is coherent in that limit.

The form of $F(x)$ near $x=1$ can be read from (3.16) or (3.17). We obtain

$$F_p(x) \cong B^{-1}(1-x)^{-1+\gamma+2(1-\alpha)}, \quad (3.19)$$

$$B = \frac{\Gamma(1-\alpha)\Gamma(\gamma+2(1-\alpha))}{\Gamma(\gamma+3(1-\alpha))}.$$

It is interesting to compare this with a conjecture

of Drell and Yan³ and also Bloom and Gilman,⁵ who showed that the exponent of the asymptotic behavior of $F(x)$ near $x=1$,

$$F(x) \sim (1-x)^n, \quad (3.20)$$

is correlated with the asymptotic q^2 dependence of the elastic form factor $F_1(q^2)$,

$$F_1(q^2) \sim (-1/q^2)^{(n+1)/2}. \quad (3.20a)$$

A further analysis within the framework of our quark model (see Appendix D) reveals that the behavior (3.20) of $F(x)$ near $x=1$ is related, not to the elastic form factor, but rather to some average of the form factors $\langle G(q^2) \rangle_{av}$ of inelastic scattering leading to states of low excitation energies W [$W^2 - M^2 < (1-x)Q^2$]. It is this average which should figure at the left-hand side of (3.20a). However, it is reasonable to expect that the q^2 dependence of the form factors of lowly excited states are not very different from the elastic one, namely, $F_1(q^2) \sim q^{-4}$. Experimental evidence (see Ref. 4) has borne this out. We therefore conclude that $n=3$. This establishes another connection between constants,

$$-1 + \gamma + 2[1 - \alpha(0)] = 3. \quad (3.20b)$$

With $\alpha(0) = \frac{1}{2}$ from Regge considerations, the number of free parameters is now reduced to one only.

To extract $W_1(q^2, \nu)$, we have to calculate the cross sections for backward scattering. In the scaling limit we get a relation between the two structure functions. From the direct calculation we have found

$$2M W_1^{p,n}(q^2, \nu) = \sum_{i=1}^3 e_i^2 G_i^{p,n}(x). \quad (3.21)$$

Therefore, by combining (3.21) with (3.16), we get a relation

$$2M x W_1(q^2, \nu) = \nu W_2(q^2, \nu). \quad (3.22)$$

It follows from (3.22) that the ratio of the probability for longitudinal photon absorption to that for transverse photons is

$$R = Q^2/\nu^2 = x 2M \nu^{-1}, \quad (3.23)$$

which is vanishing in the ideal limit when x is fixed, and $\nu \rightarrow \infty$. For finite q^2 and ν , Eq. (3.23) is compatible with the data and provides some evidence for the spin- $\frac{1}{2}$ nature of the nucleon constituents.

We now come to the Regge considerations which will determine $\alpha(0)$. We base our considerations on ideas put forward by Harari.⁶ Let us look at the limit of $F_{p,n}^v(x)$ and $F^c(x)$ for $x=0$. The functions $F_{p,n}(x)$ correspond to the amplitudes of a reaction between the virtual light quantum q_μ and the nucleon. By introducing the variable $\omega = x^{-1} = 2M\nu/Q^2$, it is seen that the limit $\omega \rightarrow \infty$ is equivalent to the

limit of large laboratory energy ν with fixed squared momentum transfer Q^2 . This corresponds to the Regge limit $\nu \rightarrow \infty$, for which we expect a dependence $\nu^{1-\alpha_K(0)}$ where $\alpha_K(0)$ is the value at $t=0$ of the Regge trajectory of the exchanged particle. The core contribution F^c becomes constant for $\omega \rightarrow \infty$, suggesting it to be the "diffractive" part of the scattering with $\alpha(0)=1$. The valence contribution F^v is different for the proton and for the neutron. In fact, the cross-section difference between neutron and proton $F_p^v - F_n^v = \frac{1}{3}F_p^v$ should be mediated by the exchange of a meson with the quantum numbers $C=1, P=(-)^J, I=1$ which are those of the A_2 meson. The trajectory of these mesons at $t=0$ has the value $\alpha(0)=\frac{1}{2}$. Hence we may use this relation at least for the limit $x \rightarrow 0$. We adopt the simplest generalization of this result by extending the validity of (2.5) to all values of x .

The assignment of the valence-quark scattering as nondiffractive and the core scattering as diffractive can be used to localize the different quarks within the nucleon. It is known that the nondiffractive scattering is mostly "peripheral," taking place near the radius R of the nucleon, whereas the diffractive scattering (shadow scattering) comes from all impact parameters between zero and R . Hence we may localize the valence quarks at the surface, and the core-quark pairs anywhere in the interior of the nucleon.

Several sum rules can be derived from our expression for $F_{p,n}(x)$. We get the integral

$$\begin{aligned} I_1^{p,n} &= \int_0^1 F_{p,n}(x) dx \\ &= \sum_{i=1}^3 e_i^2 \int_0^1 x G_i^{p,n}(x) dx = \bar{e}^2. \end{aligned} \quad (3.24)$$

This rule can be interpreted by observing that

$$\int_0^1 x \sum_{i=0}^3 G_i^{n,p}(x) dx = 1, \quad (3.25)$$

this being the expectation value of the total momentum in units of P . Hence we may consider I_1 to be an average squared charge of the partons weighed by their momenta. Another integral is

$$I_2^{n,p} = \int F_{n,p}(x) \frac{dx}{x} = \sum_{i=1}^3 e_i^2 \int G_i^{n,p}(x) dx. \quad (3.26)$$

It represents the sum of the squared charges of all partons. Since the number of partons goes like $\ln(P/M)$, this integral diverges for $P \rightarrow \infty$. The difference

$$I_2^p - I_2^n = \sum_{i=1}^3 e_i^2 \int [G_i^p(x) - G_i^n(x)] dx$$

does not diverge. We conclude from (2.6) and (2.9) that

$$I_2^p - I_2^n = e_1^2 - e_2^2 = \frac{1}{3}. \quad (3.27)$$

This very simple and definite sum rule is based upon our most radical simplification: the assumption that the core carries vacuum quantum numbers so that the isotopic spin of the nucleon is completely carried by the valence quarks.

C. Comparison of the Model Predictions with the MIT-SLAC Experiment

We expect on very general grounds that scaling holds in the limit $Q^2, \nu \rightarrow \infty$. Assuming a small value of R , the quantity νW_2 was found to roughly fall on a universal curve as a function of a single variable $x = Q^2/2M\nu$. The scaling of νW_2 was found to be improved, particularly for smaller values of Q^2 by another choice of the scaling variable,

$$x' = \frac{Q^2}{2M\nu + M^2}. \quad (3.28)$$

One observes that x' and x are identical in the infinite limit. Empirically, the new variable x' allows a better determination of the scaling function νW_2 from the data at finite Q^2 .

Bloom and Gilman⁵ discuss the theoretical significance of the new variable in terms of finite-energy sum rules. The parton model contains many reasons for expecting a deviation from the exact scaling behavior of the kind indicated by (3.28), particularly for smaller Q^2 values. The scattering becomes coherent for Q^2 comparable to the size of the nucleon. Therefore, particle correlations may play an important role. In addition, a smooth cut-off function $f(k^2)$ for the transverse momentum distribution gives corrections to the scaling variable x depending on the dimensional parameter $\langle k^2 \rangle$. Scaling sets in much faster than we would expect in any currently discussed theoretical model. We cannot give any reasons for this in our model except for a suggestion recently made by Lee.⁷ We will take the point of view that the theory predicts the scaling function in the ideal limit; the variable x' is used to provide a smooth extrapolation of the function to finite data.

Let us compare the experimental scaling function $F^p(x)$ with the predictions of the relativistic quark model. We set $\alpha(0)$ equal to $\frac{1}{2}$, which is the accepted value of the intercept of the A_2 and P' trajectories. Then Eq. (3.20) gives $\gamma=3$. We are left with the only free parameter g , which must lie between 0 and 3.

Figure 1(a) shows that a very good fit is obtained with $g=1$. It is surprising that the adjustment of one constant only yields a function which is so close to the observed values in the whole observed region. The figure $g=1$ must be interpreted by stating that there are twice as many gluons as there are

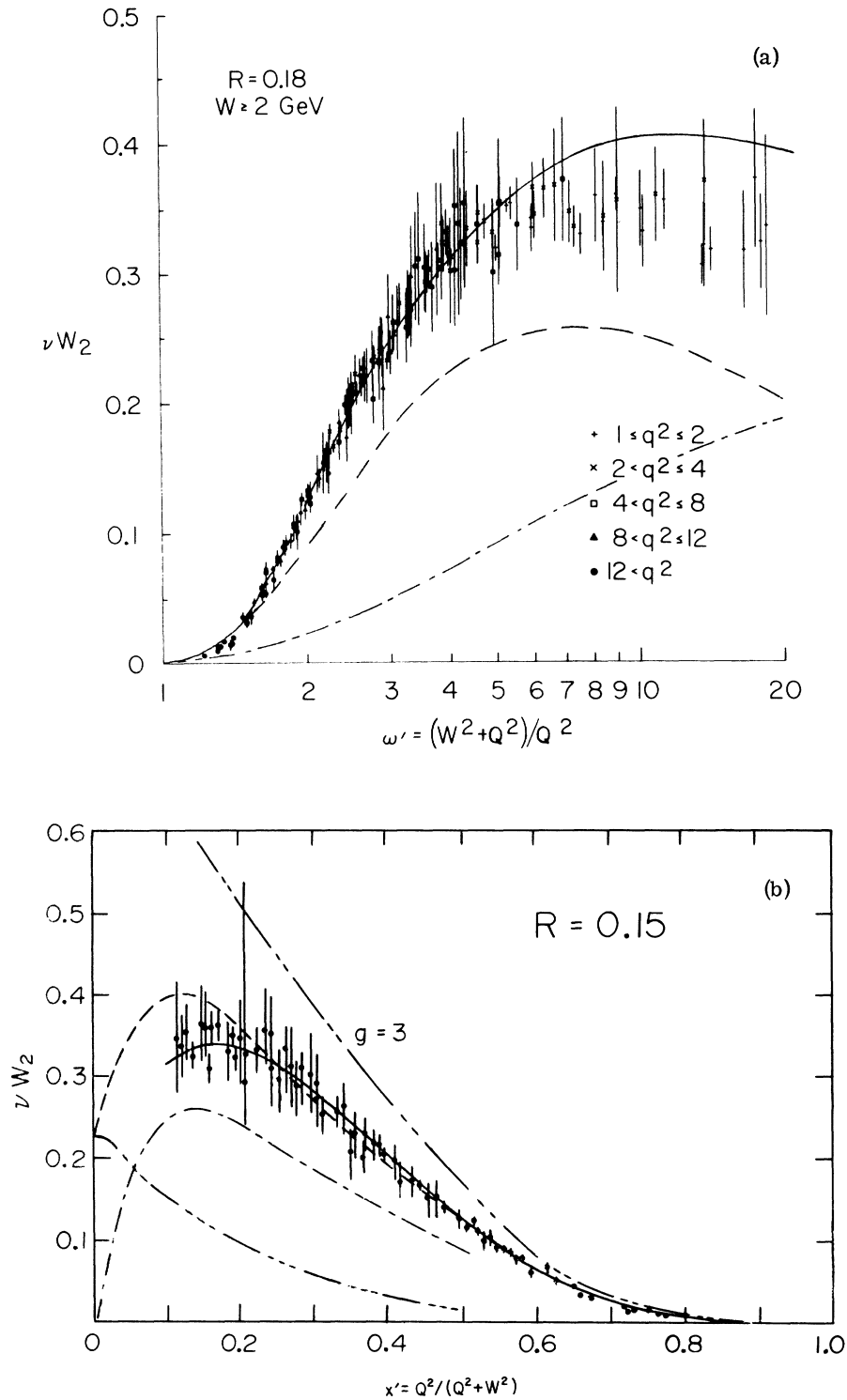


FIG. 1. (a) The inelastic structure function νW_2 as plotted versus ω' . The solid line is a fit with $\alpha(0) = \frac{1}{2}$, $\gamma = 3$, and $g = 1$. The dashed line is the valence-quark component, the dotted-dashed line is the core contribution. (b) νW_2 as a function of x' . The solid line is the best experimental fit. The dashed line is our best fit. We plotted the two components of the structure function separately. The dash-dot line is the valence-quark, the dash-dot-dot-dot line is the core contribution. The curve with $g = 3$ is too large, particularly for smaller x' .

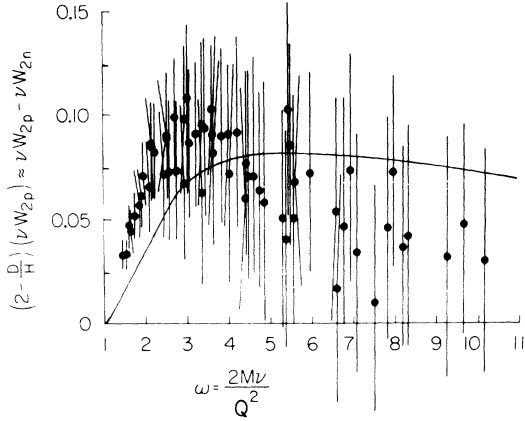


FIG. 2. The proton-neutron difference as a function of ω .

quark-antiquark pairs in the core. Figure 1(b) exhibits the separated contributions of valence and core quarks. The figure also shows the curve for $g=3$, which would be valid if there were no gluons. For small x it is too large by a factor of 2. The valence quarks are dominant for larger values of x . The difference $F^p - F^n$ and the ratio F^n/F^p of the scaling function for protons and neutrons are plotted in Figs. 2 and 3, respectively. It was convenient here to use the variable $\omega = x^{-1}$. The experimental values of F^n are very preliminary, and it is not clear at this time whether the model prediction of $\frac{2}{3}$ for the ratio near $\omega \sim 1$ is borne out or not.

Let us compare the values of the integrals I_1^p and I_1^n as defined by (3.24). Inserting $g=1$, $\alpha(0)=\frac{1}{2}$, and $\gamma=3$ into (3.19), we get

$$I_1^p = \int_0^1 F^p(x) dx = 0.16, \quad I_1^n = \int_0^1 F^n(x) dx = 0.12.$$

This compares satisfactorily with the integrals over the observed values⁴ which are known only for $x > 0.08$. They are

$$\int_{0.08}^1 F^p(x) dx \sim 0.14, \quad \int_{0.08}^1 F^n(x) dx \sim 0.10. \quad (3.29)$$

The situation with the difference $I_2^p - I_2^n$ (3.27) is less satisfactory. This value does not depend on the choice of constants in our model and should be $\frac{1}{3}$. It is difficult to extract the correct value from the experiment, since the behavior of $F(x)$ at small x is important. If one extrapolates the

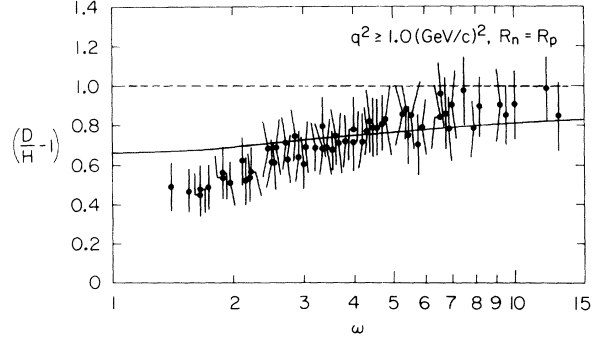


FIG. 3. The neutron-proton ratio as a function of ω .

difference $F^p - F^n$ towards $x \rightarrow 0$ with the expected asymptotic dependence $x^{-1/2}$, one obtains a rough estimate of $I_2^p - I_2^n = 0.2 \pm 0.1$. This is somewhat below the expected value. It is not clear, however, whether the extrapolation is correct. The leading Regge term may not yet be dominant at $x \sim 0.08$. If this were so, our assumption of the validity of $\psi(x) = x^{1/2}$ in (2.2) for the whole region $0 < x < 1$ would be a qualitative approximation only.

IV. SPIN DEPENDENCE OF INELASTIC ELECTRON-NUCLEON SCATTERING

Spin-dependent effects⁸⁻¹⁰ in deep-inelastic electron- (or muon-) proton scattering provide an important test of any parton model. Let us consider the scattering of a polarized electron beam with a polarized proton target. The particles are polarized along the direction of motion. We compare the cross sections for the case of parallel and antiparallel spin of the colliding particles. The measured asymmetry is defined by

$$A = \frac{d\sigma^{\uparrow\downarrow} - d\sigma^{\uparrow\uparrow}}{d\sigma^{\uparrow\downarrow} + d\sigma^{\uparrow\uparrow}}. \quad (4.1)$$

$d\sigma^{\uparrow\uparrow}$ is the cross section when the spins of electron (muon) and proton are parallel and along the direction of motion of the incident electron (muon); $d\sigma^{\uparrow\downarrow}$ is the cross section for antiparallel spins. Summation over the final electron (muon) spin and the final hadronic states is understood in Eq. (4.1).

First, we review the kinematics of spin-dependent inelastic electron-proton scattering. The spin dependence of the differential cross sections is given by

$$\frac{d^2\sigma^{\uparrow\downarrow}}{d\Omega dE_2} - \frac{d^2\sigma^{\uparrow\uparrow}}{d\Omega dE_2} = \frac{\alpha^2}{\pi} \frac{E_2}{ME_1} \frac{1}{Q^2} [(E_1 + E_2 \cos\theta)d(q^2, \nu) + (E_1 - E_2 \cos\theta)(E_1 + E_2)Mg(q^2, \nu)], \quad (4.2)$$

where E_1 and E_2 are the initial and final electron energies, as viewed in the laboratory frame, and θ is the electron scattering angle. Spins line up as defined above. The electron mass is neglected in Eq. (4.2).

$d(q^2, \nu)$ and $g(q^2, \nu)$ are the structure functions in the spin-dependent current commutator of the electromagnetic current sandwiched between proton states with covariant spin ξ_μ :

$$iW_{\mu\nu}^A(P, q) = \frac{1}{2} \int d^4x e^{i\alpha x} \{ \langle P, \xi | [j_\mu(x), j_\nu(0)] | P, \xi \rangle - (\xi \rightarrow -\xi) \}, \quad (4.3)$$

with

$$W_{\mu\nu}^A(P, q) = \epsilon_{\mu\nu\rho\sigma} q^\rho \xi^\sigma d(q^2, \nu) + (\xi \cdot q) \epsilon_{\mu\nu\rho\sigma} q^\rho p^\sigma g(q^2, \nu). \quad (4.4)$$

The antisymmetric tensor amplitude $W_{\mu\nu}^A$ contains the spin dependence which is linear in ξ_μ .

The asymmetry at a given angle θ is

$$\frac{d\sigma^{\uparrow\downarrow} - d\sigma^{\uparrow\uparrow}}{d\sigma^{\uparrow\downarrow} + d\sigma^{\uparrow\uparrow}} = \pi^{-1} \frac{M^{-1}(E_1 + E_2 \cos \theta) d(q^2, \nu) + (E_1 + E_2)(E_1 - E_2 \cos \theta) g(q^2, \nu)}{4W_1(q^2, \nu) + 2 \cot^2(\frac{1}{2}\theta) W_2(q^2, \nu)}. \quad (4.5)$$

Now we calculate (4.5) in the relativistic quark model. According to our assumption, the core has vacuum quantum numbers with zero angular momentum, and the spin-unitary-spin wave function of the three valence quarks in the nucleon ground state is dictated by SU(6). We assume that this wave function, reminiscent of a nonrelativistic theory, is appropriate in relativistic models too.¹¹ The spin-unitary-spin wave function of the three valence quarks in the symmetric quark model,

$$\begin{aligned} & \frac{1}{\sqrt{18}} (2|\uparrow\uparrow\uparrow\rangle + 2|\uparrow\uparrow\downarrow\rangle + 2|\uparrow\downarrow\uparrow\rangle \\ & - |\uparrow\uparrow\downarrow\rangle - |\uparrow\downarrow\uparrow\rangle - |\downarrow\uparrow\uparrow\rangle \\ & - |\uparrow\downarrow\downarrow\rangle - |\downarrow\uparrow\downarrow\rangle - |\downarrow\downarrow\uparrow\rangle), \end{aligned} \quad (4.6)$$

describes a proton state with spin $+\frac{1}{2}$ in the z direction (this corresponds to helicity +1 for the state moving fast in the z direction).

The wave function (4.6) yields a definite prediction for the polarization when we combine it with the single-particle distribution of the model. The asymmetry is given by

$$\frac{d\sigma^{\uparrow\downarrow} - d\sigma^{\uparrow\uparrow}}{d\sigma^{\uparrow\downarrow} + d\sigma^{\uparrow\uparrow}} = \frac{\int \frac{1}{3} G_v^p(x_i) \left(\frac{d^2\sigma^{\uparrow\downarrow}}{dq^2 dx_i} - \frac{d^2\sigma^{\uparrow\uparrow}}{dq^2 dx_i} \right) dx_i}{\sum_{i=1}^3 e_i^2 \int G_i^p(x_i) \left(\frac{d^2\sigma^{\uparrow\downarrow}}{dq^2 dx_i} + \frac{d^2\sigma^{\uparrow\uparrow}}{dq^2 dx_i} \right) dx_i}, \quad (4.7)$$

$$G_v^p(x) = G_{1v}^p(x) + G_{2v}^p(x),$$

where $d^2\sigma^{\uparrow\downarrow}/dq^2 dx_i$, etc., are the pointlike cross sections for a parton with the appropriate spin dependence (spin $\frac{1}{2}$, charge e , and three-momentum $x_i \vec{P}$). Naturally, we work again in the electron-proton c.m. system at a given value of the scaling variable $x = Q^2/2M\nu$. $G_v^p(x)$ denotes the probability density to find a valence quark with three-momentum $x \vec{P}$. In Eq. (4.7) we had to form the incoherent sum of the elementary cross sections including an integral over the three-momenta

$x_i \vec{P}$ and summation over the different particle states. The factor $\frac{5}{9}$ is calculated from the explicit structure of the spin-unitary-spin wave function in Eq. (4.6).

In Appendix A we have calculated the scaling form of the structure functions

$$\lim_{Q^2 \rightarrow \infty; x \text{ fixed}} \nu [d(q^2, \nu) + M \nu g(q^2, \nu)] = \pi \frac{10}{27} G_v^p(x). \quad (4.8)$$

If we ignore every possible angular momentum complication in the relativistic ground-state structure, we get that $\nu^2 g(q^2, \nu)$ vanishes in the scaling limit

$$\lim_{Q^2 \rightarrow \infty; x \text{ fixed}} \nu^2 g(q^2, \nu) = 0. \quad (4.9)$$

In that case

$$\nu d(q^2, \nu) \rightarrow \pi \frac{10}{27} G_v^p(x). \quad (4.10)$$

Two sum rules follow from current algebra for the spin-dependent structure functions. They are some slight extensions of Bjorken's sum rule for the spin-dependent cross section.^{8,9} First, we observe that field-theoretic models with spin- $\frac{1}{2}$ fields or smooth light-cone algebra, indicate scaling behavior

$$\lim_{Q^2 \rightarrow \infty; x \text{ fixed}} \nu d(q^2, \nu) = \alpha(x) \quad (4.11)$$

and

$$\lim_{Q^2 \rightarrow \infty; x \text{ fixed}} \nu^2 g(q^2, \nu) = \beta(x). \quad (4.12)$$

Equation (4.11) implies a leading light-cone singularity $\sim \epsilon(x_0) \delta(x^2)$ in the Fourier transform of $d(q^2, \nu)$, and Eq. (4.12) is equivalent to a step-function singularity $\sim \epsilon(x_0) \theta(x^2)$ in $g(q^2, \nu)$. These observations lead to two different sum rules if the algebra of currents is extracted from the quark model,

$$\frac{1}{2\pi} \int_0^1 dx \alpha(x) = Z$$

and

$$\int_0^1 dx \beta(x) = 0. \quad (4.13)$$

Here Z is defined by the matrix element of the axial-vector current appearing in the space-space commutator of the electromagnetic current,

$$[j_i(0, \vec{x}), j_k(0)] = -2i\epsilon_{ikl} j_5^l(0) \delta^{(3)}(\vec{x}), \quad (4.14)$$

where

$$j_\mu(x) = \bar{\psi} \gamma_\mu Q \psi, \\ j_\mu^5(x) = \bar{\psi} \gamma_5 \gamma_\mu Q^2 \psi = \frac{2}{9} \bar{\psi} \gamma_5 \gamma_\mu \psi + \frac{1}{3} \bar{\psi} \gamma_5 \gamma_\mu Q \psi, \quad (4.15)$$

and

$$Q = \begin{pmatrix} \frac{2}{3} & 0 & 0 \\ 0 & -\frac{1}{3} & 0 \\ 0 & 0 & -\frac{1}{3} \end{pmatrix}.$$

Finally,

$$\langle P, \xi | j_5^\mu(0) | P, \xi \rangle = -2MZ\xi^\mu, \\ Z = \begin{cases} \bar{Z} + \frac{1}{6} |G_A/G_V| & \text{proton target} \\ \bar{Z} - \frac{1}{6} |G_A/G_V| & \text{neutron target.} \end{cases} \quad (4.16)$$

Here $|G_A/G_V| \approx 1.2$ is the ratio of β -decay coupling constants and \bar{Z} is a model-dependent isoscalar contribution. In the free-quark model,

$$Z = \begin{cases} \frac{5}{9} & \text{proton} \\ 0 & \text{neutron.} \end{cases} \quad (4.17)$$

In our quark-parton model $\beta_{p,n}(x) = 0$ and from (4.13)

$$\frac{1}{2\pi} \int_0^1 \alpha(x) dx = \begin{cases} \frac{5}{9} & \text{proton} \\ 0 & \text{neutron.} \end{cases} \quad (4.18)$$

The vanishing right-hand side of Eq. (4.18) for neutron follows from replacing the wave function (4.6) by the appropriate neutron state.

In conclusion, the quark current-algebra sum rules are identically satisfied in the model. This is not a surprise, since both approaches are essentially free-three-quark structures in the spin-dependent case if we want to calculate the Z value explicitly.

From the valence-particle momentum distribution in our model, it follows that the functional form of the scaling function $\alpha(x)$ is given by

$$\frac{1}{2\pi} \alpha(x) = \frac{5}{9} \frac{\Gamma(\gamma + 3(1 - \alpha))}{\Gamma(1 - \alpha)\Gamma(\gamma + 2(1 - \alpha))} \\ \times x^{-\alpha(0)} (1 - x)^{-1 + \gamma + 2\alpha(0)}. \quad (4.19)$$

Some remarks on the Regge asymptotics of spin dependence are appropriate here. The Pomeron-

chukon pole is decoupled from the spin-dependent amplitudes, but the cut may contribute. This cut contribution describes a spin-dependent diffractive component in the virtual photoabsorption cross section. It vanishes in our model because we did not put any angular momentum dependence in the core, which has been associated with diffractive scattering.

Also, $\beta(x) = 0$ is a consequence of the assumed simple angular momentum structure of the nucleon-bound state. In other field-theoretic models⁹ $\beta(x)$ is a nontrivial function of x reflecting complicated angular momentum effects when spins and orbits line up in a relativistic bound state.

Taking the explicit expressions for the spin-dependent structure functions, we have calculated the asymmetry (4.5) in the deep-inelastic region where $Q^2 \geq 1$ (GeV/c)² and $W \geq 2$ GeV. Figure 4 shows the asymmetry at fixed angle θ and beam energy E_1 as a function of ω . The two different curves on the same plot are asymmetries using the scaling function (4.19), $E_1 = 10$ GeV, and $\theta = 12^\circ$ and 18° .

The polarization is large and positive over a broad range of the energy loss in the laboratory system. The sign of the asymmetry is really informative; a negative value from experiment would inevitably rule out a simple quark model. It should be kept in mind that the quantitative predictions depend on our special assumption that the valence

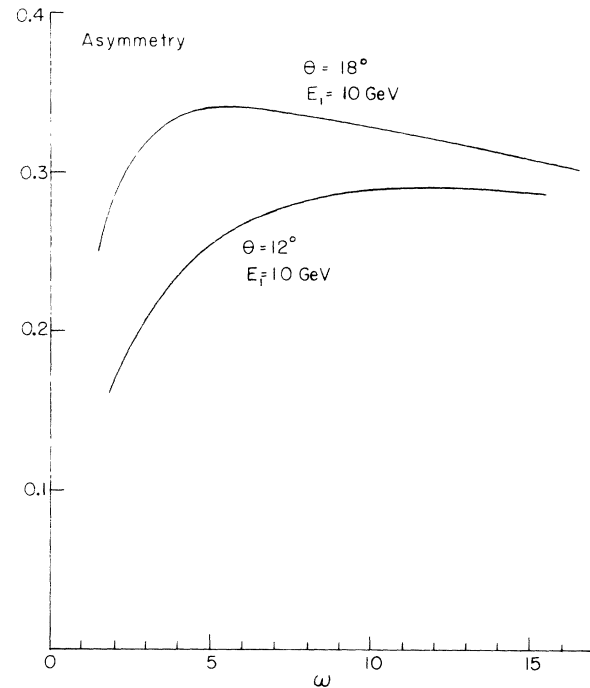


FIG. 4. The asymmetry prediction of the model at fixed incoming energy E_1 and angle θ as a function of ω .

quarks carry all quantum numbers and the core is neutral in spin and charge. The sign of the asymmetry, however, is most informative; a negative value from experiment would inevitably rule out any reasonable quark model.

V. MASSIVE $\mu^+ \mu^-$ PAIR PRODUCTION

In this section we closely follow the analysis of Drell and Yan,³ who have shown how to apply the impulse approximation to massive $\mu^+ \mu^-$ pair production in hadron-hadron collisions at high energies.

Drell and Yan argue as follows: If we want to satisfy the kinematical constraints allowing application of the impulse approximation in hadron-hadron interactions, we need to deal with interactions at high energies \sqrt{s} which absorb or produce a lepton system of large squared mass Q^2 such that the ratio Q^2/s is finite. They discuss in detail an observable process meeting this requirement,

$$p + p \rightarrow (\mu^+ \mu^-) + \text{anything}. \quad (5.1)$$

Their remarks evidently apply to any other colliding hadron pair, and to other final lepton pairs ($e^+ e^-$), $(\mu \nu)$, etc.

Drell and Yan conjecture that a process like (5.1) can be viewed in an appropriate infinite-momentum frame as the annihilation of pointlike constituents into $\mu^+ \mu^-$ pairs. On this basis, we will calculate, in the limit Q^2/s finite, $Q^2 \rightarrow \infty$, the cross section for the reaction (5.1) as an incoherent sum of parton-antiparton annihilation processes (Fig. 5). The momentum distributions of partons and antipartons can be taken from our model of the inelastic lepton-nucleon scattering.

The general expression for the cross section to form a lepton pair of squared mass Q^2 is

$$\frac{d\sigma}{dQ^2} = \frac{4\pi\alpha^2}{3Q^2} \left(1 - \frac{4m_\mu^2}{Q^2}\right)^{1/2} \left(1 + \frac{2m_\mu^2}{Q^2}\right) \times \frac{1}{\{[s - (M_1 + M_2)^2][s - (M_1 - M_2)^2]\}^{1/2}} W(Q^2, s), \quad (5.2)$$

where a spin average is understood, and

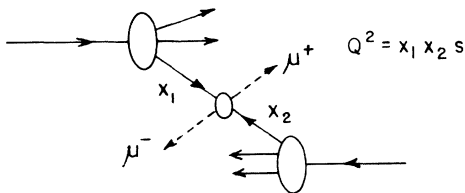


FIG. 5. Kinematics of the $\mu^+ \mu^-$ pair-production process.

$$W(Q^2, s) = -16\pi^2 E_1 E_2 \int d^4q \delta(q^2 - Q^2) \times \int d^4x e^{-iqx} \langle p_1 p_2(\text{in}) | j_\mu(x) j^\mu(0) | p_1 p_2(\text{in}) \rangle. \quad (5.3)$$

In Eqs. (5.2) and (5.3) E_1 , P_1 , M_1 and E_2 , P_2 , M_2 are the energies, momenta, and masses of the two initial hadrons; m_μ is the muon mass, and $s = (p_1 + p_2)^2$. The integral over pair momenta, d^4q , is restricted to the mass hyperboloid $q^2 = Q^2$ in the high-energy limit.

We are interested in the limiting behavior of $W(Q^2, s)$ when Q^2/s is fixed and $Q^2 \rightarrow \infty$. The structure function $W(Q^2, s)$ is dimensionless; therefore, in theories in which the limiting function does not depend on characteristic dimensional parameters we expect scaling behavior,

$$\lim_{Bj} W(Q^2, s) = W(\tau), \quad (5.4)$$

with $\tau = Q^2/s < 1$. Then from Eq. (5.2) we can write the differential cross section in a simple scaling form,

$$\frac{d\sigma}{dQ^2} = \left(\frac{4\pi\alpha^2}{3Q^2}\right) \frac{1}{Q^2} \tau W(\tau). \quad (5.5)$$

In the parton model the scaling (5.5) is obtained again by applying the impulse approximation, i.e., by assuming that the annihilating partons are moving as free particles. This assumption is somewhat more far-reaching than in the case of electron scattering, since the two partons move rapidly against each other. Drell and Yan investigate the limiting scaling behavior of $W(Q^2, s)$ in a field-theoretic model with transverse momentum cutoff in the strong-interaction vertices. Future experiments should confirm or disprove Eq. (5.5) by measuring the Q^2 dependence of the cross section at different energies.

After these general remarks we calculate $W(Q^2, s)$ for reaction (5.1) in the relativistic quark model. The matrix element for annihilation of a quark-antiquark pair becomes

$$\begin{aligned} (-) \int d^4q \delta(q^2 - Q^2) \int d^4x e^{-iqx} \langle k_1 k_2 | j_\mu(x) j^\mu(0) | k_1 k_2 \rangle \\ = \frac{e_i^2}{16\pi^2 k_{10} k_{20}} \delta(x_1 x_2 - \tau), \end{aligned} \quad (5.6)$$

where a spin average over the particles is understood, e_i^2 is the charge squared of an individual quark (of type i) measured in the electron units, and x_1 and x_2 are the fractions of the quarks' respective proton momenta. As expected, W depends only on the scaling variable τ . The argument of the δ function indicates that we have used the high-energy approximation for the momenta. Indeed, in

the c.m. system of the two colliding protons,

$$\vec{k}_1 = x_1 \vec{P},$$

$$\vec{k}_2 = -x_2 \vec{P},$$

and

$$Q^2 = (k_1 + k_2)^2 \simeq (x_1 + x_2)^2 \frac{1}{4} s - (x_1 - x_2)^2 \frac{1}{4} s = x_1 x_2 s. \quad (5.7)$$

The differential cross section (5.2) now assumes the simple form in the scaling limit,

$$\frac{d\sigma}{dQ^2} = \left(\frac{4\pi\alpha^2}{3Q^2} \right) \frac{1}{Q^2} \int_0^1 dx_1 \int_0^1 dx_2 \delta(x_1 x_2 - \tau) \times \left[\sum_i e_i^2 G_i'(x_1) G_i''(x_2) \right], \quad (5.8)$$

where $G_i'(x)$ and $G_i''(x)$ are the probabilities to find a quark or an antiquark of type i with momentum $x\vec{P}$. The functions $G_i(x)$ introduced in (2.7) comprise both particles and antiparticles. In terms of those expressions, we easily find

$$G_i'(x) = G_{iv}(x) + \frac{1}{2} G_{ic}(x),$$

$$G_i''(x) = \frac{1}{2} G_{ic}(x), \quad (5.9)$$

since antiparticles are found only in the core.

$$F_E(\tau) = \int_0^1 dx_1 \int_0^1 dx_2 \frac{1}{2} \left[\theta \left(x_1 - \frac{2Mq_{L\min}}{s} \right) + \theta \left(x_2 - \frac{2Mq_{L\min}}{s} \right) \right] \delta(x_1 x_2 - \tau) \left[\sum_i e_i^2 G_i'(x_1) G_i''(x_2) \right]. \quad (5.11)$$

In Eq. (5.11) the integrand has been symmetrized in x_1 and x_2 .

Figure 6 shows the differential cross section as calculated from Eq. (5.11). We have plotted the cross section with $g=3$ (no gluon) and with the g value which corresponds to the best fit for the inelastic electron scattering. Some remarks are appropriate here:

(a) A large contribution to the cross section comes from the annihilation of a valence quark with an antiquark in the core and vice versa. The reason for this is that in the relevant kinematic region x lies between 1 and $\frac{1}{3}$, and in that range of the scaling variable there are many more valence quarks than core quarks [see Fig. 1(b)].

(b) In Fig. 6 we have plotted the differential cross sections for $s=900$ (GeV)² and $s=2500$ (GeV)² in the energy range of the new accelerators (National Accelerator Laboratory and CERN Intersecting Storage Rings). The cross sections have been calculated with the same momentum resolution as at $s=60$ (GeV)², setting $q_{L\min}$ equal to 12 GeV/ c .

The derivation of (5.8) is transparent physically. The differential cross section is the incoherent sum of elementary annihilation processes weighted by the probabilities to find a quark of type i with momentum $x_1 \vec{P}$ to annihilate with an antiquark of momentum $-x_2 \vec{P}$. The elementary cross section is calculated from Eqs. (5.2), (5.3), and (5.6).

The data¹² to which we want to compare Eq. (5.8) were obtained by taking a limited cut of the events leading to a given lepton pair squared mass of Q^2 . Only those events were detected for high-energy protons incident on a uranium nucleus leading to muon pairs of total momentum $Q \geq 12$ GeV/ c and emerging with $Q_1/Q \leq \frac{1}{18}$ in the laboratory system. Therefore, these experimental resolution functions must be introduced before a detailed comparison can be made. We follow Drell and Yan's method of taking care of that cut and introduce a longitudinal momentum cutoff corresponding to $q_{L\min} = 12$ GeV/ c . The experimental constraint that $q_L > q_{L\min}$ can be expressed as a step function to be inserted directly into (5.8),

$$\left(\frac{d\sigma}{dQ^2} \right)_E = \frac{4\pi\alpha^2}{3Q^2} \frac{1}{Q^2} F_E(\tau), \quad (5.10)$$

with

(c) The total cross section at 29.5 GeV incident proton energy [$s=60$ (GeV)²] in our model is 1.9×10^{-33} cm², compared to the experimental number $(2.9 \pm 0.3) \times 10^{-33}$ cm². It is no surprise that our total cross section is somewhat smaller since a large contribution to the total cross section comes from the relatively small Q^2 region where the model curve is below the data points.

(d) In our calculation we concentrated on the simple annihilation process and ignored every other diagram [e.g., parton + parton (antiparton) - parton + parton (antiparton) + $\mu^+ \mu^-$ pair].

VI. HIGH-ENERGY INELASTIC NEUTRINO-NUCLEON SCATTERING

High-energy inelastic neutrino-nucleon processes provide an independent test of the theoretical developments for deep-inelastic electron-nucleon scattering.¹³ The detailed comparison of the model with available neutrino data will be published elsewhere. Here we review only some of the results which are relevant in comparison with electroproduction.

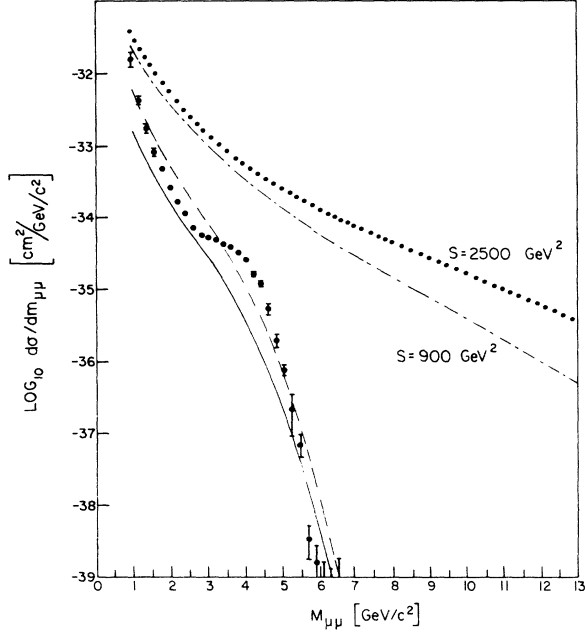


FIG. 6. The $\mu^+\mu^-$ pair production cross section as a function of the invariant mass of the $\mu^+\mu^-$ pair. The solid line is $g=1$, the dashed line is $g=3$. The dotted line corresponds to $s=2500$ (GeV) 2 , the dashed-dotted one is $s=900$ (GeV) 2 ; both are plotted with $g=1$.

In notation we follow Bjorken and Paschos, who have derived general sum rules in the framework of the parton model.

The kinematics of the process is shown in Fig. 7, where

- k_1 =four-momentum of neutrino,
- k_2 =four-momentum of muon,
- $q=k_1-k_2$ =momentum transferred from leptons to hadrons,
- $\nu=E_1-E_2$ =energy transfer in laboratory frame,
- P =four-momentum of target nucleon,
- θ =angle of produced muon relative to incident neutrino,
- $Q^2=-q^2=4E_1E_2\sin^2(\frac{1}{2}\theta)$.

For the hadronic current operator we use the Cabibbo current

$$j_\mu = (V_\mu - A_\mu)^{\Delta s=0} \cos\theta_C + (V_\mu - A_\mu)^{|\Delta s|=1} \sin\theta_C. \quad (6.1)$$

The normalization is such that in the quark model

$$j_\mu = \bar{\psi} \gamma_\mu (1 - \gamma_5) (\mathcal{X} \cos\theta_C + \lambda \sin\theta_C), \quad (6.2)$$

where \mathcal{P} , \mathcal{X} , λ are the quark field operators. It is natural to describe the process in terms of cross sections corresponding to the three helicity states of the virtual W exchanged between the leptons and hadrons: right-handed (R), left-handed (L), and scalar (S).

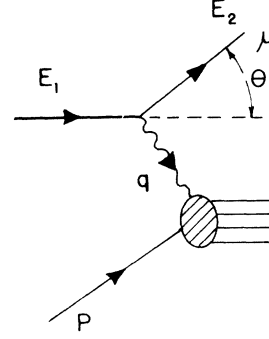


FIG. 7. Kinematics of inelastic neutrino-nucleon scattering.

We write, for high energies only,

$$\frac{d^2\sigma}{dQ^2 d\nu} = \frac{G^2}{2\pi} \frac{E_2}{E_1} \beta(Q^2, \nu) \left[1 + \frac{\nu}{E_2} (L) - \frac{\nu}{E_1} (R) \right], \quad (6.3)$$

where

$$(L) = \frac{\sigma_L}{\sigma_R + \sigma_L + 2\sigma_S} \ll 1, \quad (R) = \frac{\sigma_R}{\sigma_R + \sigma_L + 2\sigma_S} \ll 1. \quad (6.4)$$

σ_R , σ_L , and σ_S are the appropriate helicity cross sections for "virtual W "-nucleon absorption, defined analogously to the Hand cross sections used in electroproduction. $\beta(Q^2, \nu)$ has the same definition as $W_2(Q^2, \nu)$ in electroproduction and can be expressed in terms of the helicity cross sections as

$$\beta(Q^2, \nu) = \frac{1}{2\pi} \frac{Q^2}{\nu} \frac{1}{1 + Q^2/\nu^2} \left(1 - \frac{Q^2}{2M\nu} \right) (2\sigma_S + \sigma_R + \sigma_L). \quad (6.5)$$

Without the high-energy approximation in (6.3), we write

$$\frac{d^2\sigma}{dQ^2 d\nu} = \frac{G^2}{2\pi} \frac{E_2}{E_1} \beta(Q^2, \nu) \left[1 - \frac{Q^2}{4E_1E_2} + \frac{\nu^2 + Q^2}{2E_1E_2} (R + L) + \frac{(E_1 + E_2)(\nu^2 + Q^2)^{1/2}}{2E_1E_2} (L - R) \right]. \quad (6.6)$$

The muon mass is neglected in Eq. (6.6).

We again assume that the neutrino is scattered incoherently by each parton in a pointlike fashion. For spin- $\frac{1}{2}$ quarks, only σ_L contributes to the neutrino cross section as $\nu, Q^2 \rightarrow \infty$; $\sigma_R = \sigma_S = 0$ in this limit. Similarly, for spin- $\frac{1}{2}$ antiquarks, only σ_R is nonvanishing in the asymptotic limit.

For neutrino-induced reactions, we find

$$\nu\beta(R) = 2xG_1'(x), \quad (6.7)$$

$$\nu\beta(L) = 2x[G_2'(x) \cos^2\theta_C + G_3'(x) \sin^2\theta_C]. \quad (6.8)$$

The G' functions are defined in (5.9). In our model $\nu\beta(R)$ receives contributions only from the core with antiquarks present, whereas $\nu\beta(L)$ has both valence-quark and core-quark contributions. The scale-invariant form of $\nu\beta(R)$ and $\nu\beta(L)$ allows us to write (6.3) in the simple form

$$\sigma_{\text{tot}} = \frac{G^2 M E_1}{\pi} \int_0^1 dx \left(\frac{\nu\beta_p + \nu\beta_n}{2} \right) \left(\frac{1}{2} + \frac{1}{2} \langle L \rangle - \frac{1}{6} \langle R \rangle \right), \quad (6.9)$$

where $\langle R \rangle$ and $\langle L \rangle$ imply that the appropriate averages over x have been taken. This formula exhibits the linear dependence of the total neutrino-nucleon cross section on the incident neutrino energy. In (6.9) we included an average over protons and neutrons in the target.

It is important to recognize that the experiment¹⁴ has been done at moderately high energies in a bubble chamber, so a non-negligible part of the inelastic events is not "deep-inelastic." In deriving Eq. (6.9), the scaling functions were used in the whole inelastic phase space. The linear E dependence of the total cross section in the CERN experiment is remarkable, and we are tempted to compare it with the quark model.

Using the definite single-particle distributions of the model, we have the following expressions for neutrons and protons:

$$\begin{aligned} \nu\beta_p(R) &= \frac{1}{3}g(1-x)^{-1+\gamma+3\alpha(0)}, \\ \nu\beta_n(R) &= \nu\beta_p(R), \\ \nu\beta_p(L) &= 2 \cos^2 \theta_c \frac{\Gamma(\gamma+3(1-\alpha))}{\Gamma(1-\alpha)\Gamma(\gamma+2(1-\alpha))} x^{1-\alpha(0)} \\ &\quad \times (1-x)^{-1+\gamma+2\alpha(0) + \frac{1}{3}g(1-x)^{-1+\gamma+3\alpha(0)}, \\ \nu\beta_n(L) &= 2\nu\beta_p(L) - \frac{1}{3}g(1-x)^{-1+\gamma+3\alpha(0)}. \end{aligned} \quad (6.10)$$

It is straightforward to calculate the integral in the cross-section formula (6.9) using Eq. (6.10). We get

$$\sigma_{\text{tot}} = 0.55 \times 10^{-38} E_1 \text{ cm}^2/\text{nucleon} \quad (6.11)$$

to be compared with the experimental value,

$$\sigma_{\text{tot}} = (0.8 \pm 0.2) \times 10^{-38} E_1 \text{ cm}^2/\text{nucleon}. \quad (6.12)$$

In calculating Eq. (6.11), we have used $\alpha(0) = \frac{1}{2}$, $\gamma = 3$, and $g = 1$. The detailed analysis of the model for neutrino- (antineutrino-) induced reactions will be published in a separate paper.

VII. CONCLUSIONS AND SPECULATIONS

The considerations in this paper show that the inelastic scattering of electrons by nucleons in the limit of large momentum transfer q and energy loss ν , but finite ratio $\omega = 2M\nu/Q^2$ can be qualitatively reproduced by a model in which the nucleon

in the center-of-mass system is represented as an assembly of free quarks, with fractional charges and unity form factor. The nucleon contains the three well-known quarks of the naive quark model (valence quarks) and, in addition, an undetermined number of quark-antiquark pairs. The longitudinal momentum distribution of the pairs is proportional to the relativistic phase space ($\sim dP/P_0$) restricted by the condition of small transverse momentum. The momentum distribution of the "valence quarks" is $dP/P_0^{1/2}$, suggested from Regge considerations. The agreement can be made quantitative by adding uncharged "gluons," with a phase-space momentum distribution. The model, with its constants adjusted to agree with the electron scattering experiments, also reproduces the observed total cross section for inelastic neutrino scattering and gives the general features of the presently observed high-energy $\mu^+ \mu^-$ pairs produced by proton-nucleon collisions. It predicts a scaling property of this latter process, namely, the appearance of a structure function depending only on the ratio s/q^2 [see Eq. (5.4)].

One special feature of our hypothesis is the assumption that the three valence quarks alone carry the specific quantum numbers of the nucleon; the pair core has vacuum quantum numbers. This assumption was made for the sake of simplicity. It has important consequences in regard to the predictions of the difference between neutron and proton scattering cross sections and the predictions of Sec. IV about the dependence of the scattering on the relative spin directions of the partners. Future experiments will show whether this assumption is sensible or not.

The proposed model implies that the inelastic scattering of an electron by a nucleon is an elastic scattering of the electron by a single quark. The applicability of the free-quark model (impulse approximation) to presently available energies implies that the bindings between the quarks are weak compared to the applied momentum transfers. Hence, one would predict that single free quarks be produced in the process. The evidence against this prediction is overwhelming.

One may conclude from this failure that the proposed quark model is invalid and its agreement with experiments is purely accidental. However, if the predictions of the model will be established by further experiments, one may be forced to conclude that the quark model in its present form is a reasonable though incomplete model of reality in the sense that the quark concept in its present form may be only partially appropriate for the description of what goes on within a nucleon. If one wants to retain the concept, one would have to introduce a new principle which forbids quarks to leave the

bounds of a hadron, except in pairs with antiquarks or in triplets. The effect on the dynamics of a single quark would be reminiscent of a potential tending to infinity for large distances away from the hadron, like an oscillator potential. When the single quark is forced by the quasi-potential to change its momentum, some quark-antiquark pairs would be created (bremsstrahlung), enabling the quark to grab an antiquark and to leave the nucleon.

The same difficulty appears when one tries to apply the concepts of our model to the hadron production by electron-positron collision experiments. One would conclude that all the electron pair can do is to create a quark pair; the two partners would move in opposite directions until they reach the limits of the aforementioned quasi-potential. Then additional quark pairs are produced, which would allow the appearance of hadrons as the end product of the process. The total cross section for such hadron production should be the quark pair-production cross section, summed over the three quark types. This is two-thirds times the muon pair-production cross sections. It should be valid only in the limit of high energy ($E \gg M$). Actually, this result is not far from the value obtained in the Frascati experiments.¹⁵

The idea of an effective oscillator potential acting upon the constituents of hadrons has also appeared in different contexts. There are recent attempts to describe hadron dynamics with quark oscillators, and the equidistant resonance spectrum resulting from the Veneziano approach¹⁶ points to a system of harmonic oscillators. Are these oscillators connected with the nonexistence of single quarks outside the hadron?

Note added in proof. A recent, more complete, analysis of the data obtained by the authors of Ref. 4, taking into account all necessary correc-

tions, has revealed that the values for W_2^n/W_2^p shown in Fig. 3 are too high for $\omega \rightarrow 1$. The intercept at $\omega = 1$ seems to be definitely lower than $\frac{2}{3}$ and probably lower than $\frac{1}{2}$. This experimental result would raise considerable doubt as to the validity of our assumptions. Within the framework of our picture of valence and core quarks, a low ratio of W_2^n/W_2^p invalidates the assumption that the three valence quarks have the same momentum distribution $G(x)$. J. I. Friedman suggested that the following assumption would give values of W_2^n/W_2^p lower than $\frac{2}{3}$: One would have to assume that, in the proton, the \mathcal{P} -type valence quarks have a higher $G(x)$ than the \mathcal{N} -type ones for $x \rightarrow 1$. In the neutron the situation would be reversed according to SU(2) symmetry. In the extreme case of $G_2^p(1)/G_1^p(1) = 0$, W_2^n/W_2^p would assume the value $\frac{1}{4}$ at $x = 1$. A value lower than $\frac{1}{4}$ is excluded by any quark model. [See O. Nachtmann, Orsay Report No. LPTHE 71/29 (unpublished).] It should be pointed out that a replacement of the valence neutron quark distribution $\sqrt{x}(dx/x)$ inside the proton by $(1-x)\sqrt{x}(dx/x)$ reproduces the new data and does not give rise to any qualitative changes in the other predictions made in this paper. However, it would be difficult to find a simple explanation for such pronounced asymmetries in the distributions of the valence quarks.

ACKNOWLEDGMENTS

The authors would like to express their deep appreciation for help, stimulation, and criticism to R. Feynman, J. Bjorken, S. Drell, J. Friedman, H. Kendall, and M. Breidenbach. One of us (J. K.) would like to express his gratitude for the hospitality he enjoyed at the Center for Theoretical Physics at MIT.

APPENDIX A

First we derive expressions for the spin-averaged structure functions. In the electron-proton c.m. system, we write (3.1) in terms of these structure functions as follows:

$$d\sigma = \frac{1}{4}e^4q^{-4} \frac{8\pi M}{k_1 \cdot P} \left[-q^2 W_1(q^2, \nu) + \left(\frac{2P \cdot k_1 P \cdot k_2}{M^2} + \frac{1}{2}q^2 \right) W_2(q^2, \nu) \right] \frac{d^3k_2}{(2\pi)^3 2E_2}. \quad (\text{A1})$$

The electron mass is neglected in (A1). It is straightforward to calculate the limiting behavior of $d\sigma$ when the three-momentum P of the proton goes to infinity, but q^2 and ν are fixed at large values. In the $P \rightarrow \infty$ limit (with fixed q^2 and ν), the scattering angle is small ($\theta \rightarrow 0$) which makes it plausible that W_2 is the leading term in the asymptotic expression,

$$d\sigma \underset{P \rightarrow \infty}{\sim} \frac{P}{M} 8\alpha^2 q^{-4} W_2(q^2, \nu) d^3k_2. \quad (\text{A2})$$

We evaluate the limiting behavior of the cross section in the parton model in which the probability of electron scattering in a given range is constructed from elementary processes. Suppose that a quark of type i with momentum $P_i = x_i P$ and charge e_i (in electron units) scatters the electron in range d^3k_2 .

The cross section for this elementary process with the same q as in (A2) is given by

$$d\sigma_i(x_i) = \frac{1}{4} e^4 e_i^2 q^{-4} \frac{16\pi}{k_1 \cdot P_i} \delta(2q \cdot P_i + q^2) \times (\frac{1}{4} q^4 + 2P_i \cdot k_1 P_i \cdot k_2 + \frac{1}{2} \mu^2 q^2) \frac{d^3 k_2}{(2\pi)^3 2E_2}. \quad (\text{A3})$$

In the $P \rightarrow \infty$ limit the δ function in (A3) becomes

$$\delta(2q \cdot P_i + q^2) = \frac{1}{2M\nu} \delta(x_i - x), \quad (\text{A4})$$

$$x = \frac{Q^2}{2M\nu},$$

which tells us that the electron is forced to select a quark with $x_i = x$ by energy-momentum conservation.

Asymptotically we find

$$d\sigma_i(x_i) \rightarrow \frac{P}{M} 8\alpha^2 q^{-4} e_i^2 \frac{x_i}{\nu} \delta(x_i - x) d^3 k_2. \quad (\text{A5})$$

In the physical scattering process we have to multiply $d\sigma_i(x_i)$ by $G_i(x_i)$ which is the probability function to find a quark of type i with momentum $x_i P$. Comparison of (A2) with (A5) gives the contribution of quarks of type i to $\nu W_2(q^2, \nu)$ for fixed x with variable x_i :

$$\nu W_2^{(i)}(q^2, \nu) = e_i^2 x_i \delta(x - x_i) G_i(x_i). \quad (\text{A6})$$

We get the complete structure function by integrating over x_i and introducing a summation over i ,

$$\nu W_2(q^2, \nu) = x \sum_i e_i^2 G_i(x). \quad (\text{A7})$$

This is the formula we have used in Eq. (3.16).

Next, we extract $W_1(q^2, \nu)$. The asymptotic limits of the cross sections can be calculated in backward scattering $\theta = \pi$. In that special case $W_1(q^2, \nu)$ is the dominant term in the phenomenological expression,

$$d\sigma \underset{P \rightarrow \infty}{\sim} \frac{1}{4} e^4 q^{-4} \frac{8\pi}{k_1 \cdot P} Q^2 M W_1(q^2, \nu) \frac{d^3 k_2}{(2\pi)^3 2E_2}. \quad (\text{A8})$$

The same limit for a quark of type i is

$$d\sigma_i(x_i) \rightarrow \frac{1}{4} e^4 q^{-4} \frac{4\pi}{k_1 \cdot P_i} e_i^2 q^4 \delta(2P_i \cdot q + q^2) \frac{d^3 k_2}{(2\pi)^3 2E_2}. \quad (\text{A9})$$

Again, writing the δ function in the form (A4), we get by comparison

$$2M W_1^{(i)}(q^2, \nu) = e_i^2 \delta(x - x_i) G_i(x_i), \quad (\text{A10})$$

where we have weighted the contribution of $d\sigma_i(x_i)$ to (A8) by the probability function $G_i(x_i)$. After summation and integration we find

$$2M W_1(q^2, \nu) = \sum_i e_i^2 G_i(x). \quad (\text{A11})$$

Formula (A11) has been used in Sec. III to calculate the ratio for longitudinal photon absorption to that for transverse photons.

Finally, we extract the spin-dependent structure functions from the quark-parton model. The procedure is the same as before. We calculate the asymptotic form of the spin-dependent cross sections in the electron-proton c.m. system,

$$\frac{1}{2}(d\sigma^{\uparrow\downarrow} - d\sigma^{\uparrow\uparrow}) \underset{P \rightarrow \infty}{\sim} \alpha^2 P^{-1} (\pi M Q^2)^{-1} \times [d(q^2, \nu) + M\nu g(q^2, \nu)] d^3 k_2. \quad (\text{A12})$$

The structure functions $d(q^2, \nu)$ and $g(q^2, \nu)$ have been defined in Sec. IV. Equation (A12) is valid under the same conditions as the spin-averaged limits: q^2, ν are large and fixed, $P \rightarrow \infty$. Notice that the spin dependence is of order P^{-1} , but this limit is used and only used to express $d(q^2, \nu)$ and $g(q^2, \nu)$ in terms of the probability functions $G_i(x)$. After having the explicit functions, we calculate the asymmetry in a realistic kinematic region.

For a quark of type i with momentum $x_i P$ and charge e_i , the spin dependence is

$$\frac{1}{2}(d\sigma_i^{\uparrow\downarrow} - d\sigma_i^{\uparrow\uparrow}) = 4\alpha^2 P^{-1} e_i^2 Q^{-2} \delta(2P_i \cdot q + q^2) d^3 k_2. \quad (\text{A13})$$

Using (A14), we write

$$\frac{1}{2}(d\sigma_i^{\uparrow\downarrow} - d\sigma_i^{\uparrow\uparrow}) = 2\alpha^2 P^{-1} e_i^2 (M Q^2 \nu)^{-1} \delta(x - x_i) d^3 k_2. \quad (\text{A14})$$

According to our assumption, only valence quarks contribute to (A12). The wave function (4.6) dictates how to calculate the spin dependence on the three valence quarks with probability functions $G_{iv}(x_i)$. In comparison with (A12), we have to introduce $G_{iv}(x_i)$ in (A14) and use the wave function (4.6). We get

$$\frac{1}{2\pi} [\nu d(q^2, \nu) + M\nu^2 g(q^2, \nu)]_p = \frac{5}{9} G_2 \nu(x). \quad (\text{A15})$$

This form has been used in Sec. IV.

If spins line up parallel and antiparallel along the direction of motion, then it is clear from (A12) that only the $d + M\nu g$ combination can be extracted. Equation (A15) is valid for protons with the valence configuration (4.6), whereas the wave function (4.18a) for neutrons yields a vanishing coefficient on the right-hand side of (A15),

$$\nu [d(q^2, \nu) + M\nu g(q^2, \nu)]_n = 0. \quad (\text{A16})$$

Equation (A16) is a very strong conclusion, indicating that spin dependence of the scattering by neutrons should vanish in our model asymptotically.

It is not hard to show that $\nu^2 g(q^2, \nu)$ does not contribute to the scaling function in (A15),

$$\lim_{Q^2 \rightarrow \infty; x \text{ fixed}} \nu^2 g_{p,n}(q^2, \nu) = 0. \quad (\text{A17})$$

This observation has been derived from the assumption that we ignore every possible angular momentum complication in the relativistic ground-

state structure; that is, the quark spins always line up to yield the spin of the proton at rest or the proper helicity combination in the fast-moving state.

Field-theoretic models indicate that (A17) is not necessarily true in the presence of orbital angular momenta.

APPENDIX B

In this Appendix we indicate how to calculate the functional form of the single-particle distributions and the scaling form of the structure functions. The valence-quark distribution is given by

$$G_{2\nu}(x) = Z \frac{x^{1-\alpha(0)}}{(x^2 + \mu^2/P^2)^{1/2}} \sum_{k_i=0,2,\dots; l=0,1,2,\dots} \frac{(\frac{1}{3}g)^{k_1}(\frac{1}{3}g)^{k_2}(\frac{1}{3}g)^{k_3}(g')^l}{k_1!k_2!k_3!l!} I_{n-1}^{\nu}(x), \quad (\text{B1})$$

with

$$I_{n-1}^{\nu}(x) = \int \prod_{j=1}^{n-1} \frac{dx_j}{(x_j^2 + \mu^2/P^2)^{1/2}} x_1^{1-\alpha(0)} x_2^{1-\alpha(0)} \delta\left(1 - x - \sum_{j=1}^{n-1} x_j\right). \quad (\text{B2})$$

Here $n = 3 + k_1 + k_2 + k_3 + l$ stands for the total number of particles in a state with $3 + k_1 + k_2 + k_3$ quarks and l gluons; $n = 3, 4, 5, \dots$.

We introduce the representation

$$\delta\left(1 - x - \sum_{j=1}^{n-1} x_j\right) = \frac{1}{2\pi} \int \exp\left[i\left(1 - x - \sum_{j=1}^{n-1} x_j\right)\xi\right] d\xi. \quad (\text{B3})$$

Using (B3), the $(n-1)$ -dimensional integral can be carried out,

$$I_{n-1}^{\nu}(x) = \frac{1}{2\pi} \int e^{i(1-x)\xi} v^2(\xi) c^{n-3}(\xi) d\xi, \quad (\text{B4})$$

where

$$v(\xi) = \int_0^{\infty} e^{-i\xi x} \frac{x^{1-\alpha(0)}}{(x^2 + \mu^2/P^2)^{1/2}} dx \quad (\text{B5})$$

and

$$c(\xi) = \int_0^{\infty} e^{-i\xi x} \frac{1}{(x^2 + \mu^2/P^2)^{1/2}} dx \quad (\text{B6})$$

The integrals (B5) and (B6) can be obtained in closed form consulting integral tables. The calculation goes then as follows. With the help of (B4),

$$G_{2\nu}(x) = Z \frac{x^{1-\alpha(0)}}{(x^2 + \mu^2/P^2)^{1/2}} (2\pi)^{-1} \int e^{i(1-x)\xi} v^2(\xi) \left\{ \sum_{k_1, k_2, k_3, l} \frac{(\frac{1}{3}g)^{k_1}(\frac{1}{3}g)^{k_2}(\frac{1}{3}g)^{k_3}(g')^l}{k_1!k_2!k_3!l!} [c(\xi)]^{k_1+k_2+k_3+l} \right\} d\xi. \quad (\text{B7})$$

The summation over k_1, k_2, k_3, l is carried out before the integration over ξ . It is a simple exercise to sum, observing that the power of $c(\xi)$ depends only on the sum of the summation indices. This allows us to reduce the quadruple sum to a single one, if we use the simple properties of the binomial series,

$$\sum_{k_i=0,1,2,\dots; l=0,1,2,\dots} \frac{(\frac{1}{3}g)^{k_1}(\frac{1}{3}g)^{k_2}(\frac{1}{3}g)^{k_3}(g')^l}{k_1!k_2!k_3!l!} c^{k_1+k_2+k_3+l} = \sum_{n=0,1,2,\dots} \frac{(g+g')^n}{n!} c^n. \quad (\text{B8})$$

It is simple algebra to take into account that k_i , $i = 1, 2, 3$ runs over even integers. The quadruple sum in (B7) is exponentiating, and we are left with an explicit function of ξ which depends on the parameter P .

Before we integrate, the asymptotic limit $P \rightarrow \infty$ of the integrand is taken.

These instructions are complete to get the result on $G_{2\nu}(x)$:

$$G_{2\nu}(x) = Z b x^{-\alpha(0)} (1-x)^{-1+\gamma+2[1-\alpha(0)]} \quad (\text{B9})$$

with $\gamma = g + g'$. In (B9) b is an explicit function of the model parameters: $\alpha(0)$, g , and g' .

Similar procedure applies to $G_c(x)$,

$$G_{1c}(x) = Z \frac{1}{(x^2 + \mu^2/P^2)^{1/2}} \sum_{k_i=0,2,\dots;l=0,1,2,\dots} k_1 \frac{(\frac{1}{3}g)^{k_1} (\frac{1}{3}g)^{k_2} (\frac{1}{3}g)^{k_3} (g')^l}{k_1! k_2! k_3! l!} I_{n-1}^c(x), \quad (\text{B10})$$

with

$$I_{n-1}^c(x) = \int \prod_{j=1}^{n-1} \frac{dx_j}{(x_j^2 + \mu^2/P^2)^{1/2}} x_1^{1-\alpha(0)} x_2^{1-\alpha(0)} x_3^{1-\alpha(0)} \delta\left(1 - x - \sum_{j=1}^{n-1} x_j\right), \quad (\text{B11})$$

$n = 3 + k_1 + k_2 + k_3 + l$, $n > 3$. With the Fourier representation for the δ function, we write

$$I_{n-1}^c(x) = \frac{1}{2\pi} \int e^{i(1-x)\xi} v^3(\xi) c^{n-4}(\xi) d\xi. \quad (\text{B12})$$

After summation and integration we find

$$xG_{1c}(x) = Z b \frac{1}{3} g \frac{\Gamma(1-\alpha)\Gamma(\gamma+2(1-\alpha))}{\Gamma(\gamma+3(1-\alpha))} (1-x)^{-1+\gamma+3[1-\alpha(0)]}. \quad (\text{B13})$$

Z is calculated by normalizing the total probability of finding partons to one:

$$Z^{-1} = b \frac{\Gamma(1-\alpha)\Gamma(\gamma+2(1-\alpha))}{\Gamma(\gamma+3(1-\alpha))}. \quad (\text{B14})$$

Therefore, we can write (B9) and (B13) in their final form,

$$G_{2v}(x) = \frac{\Gamma(\gamma+3(1-\alpha))}{\Gamma(1-\alpha)\Gamma(\gamma+2(1-\alpha))} x^{-\alpha(0)} (1-x)^{-1+\gamma+2[1-\alpha(0)]}, \quad (\text{B15})$$

$$xG_{1c}(x) = \frac{1}{3} g (1-x)^{-1+\gamma+3[1-\alpha(0)]}. \quad (\text{B16})$$

APPENDIX C

Here we discuss the evidence for the presence of uncharged partons (gluons) within the proton in addition to the quarks.¹⁷ The conclusion is based upon the extrapolated experimental values of I_{1p} and I_{1n} [see Eq. (3.29)],

$$I_{1p} \cong 0.17 \pm 0.01, \quad I_{1n} \cong 0.13 \pm 0.01 \quad (\text{experimental}). \quad (\text{C1})$$

We use the functions defined in (2.7) and introduce the following integrals:

$$I_i = \int_0^1 x G_i^p(x) dx. \quad (\text{C2})$$

We then get from (3.24)

$$I_{1p} = \sum_i e_i^2 I_i = \frac{4}{9} I_1 + \frac{1}{9} I_2 + \frac{1}{9} I_3. \quad (\text{C3a})$$

For the neutron we get, because of isospin symmetry,

$$I_{1n} = \frac{1}{9} I_1 + \frac{4}{9} I_2 + \frac{1}{9} I_3. \quad (\text{C3b})$$

According to (C2), I_i is the expectation value of x carried by the i -type quarks. If the proton contains only quarks and no other particles, we must have

$$I_1 + I_2 + I_3 = 1. \quad (\text{C3c})$$

The set of equations (C1) and (C3a)–(C3c) yield

$$I_1 = 0.18 \pm 0.03,$$

$$I_2 = 0.06 \pm 0.03,$$

$$I_3 = 0.76 \pm 0.06.$$

This result cannot be excluded on theoretical grounds, but it seems most implausible that there should be four times as many λ quarks as \mathcal{P} quarks in the proton. Here, the number of quarks is weighted by their momentum.

The introduction of gluons changes the situation. Equation (C3c) should be replaced by

$$I_1 + I_2 + I_3 + I_0 = 1, \quad (\text{C3d})$$

where I_0 refers to the gluons. From our fit in Sec. III we obtained $g' = 2g$ which means $I_0 = 2I_3$. Using this relation, we now obtain from (C3a), (C3b), and (C3d)

$$I_1 = 0.29 \pm 0.03,$$

$$I_2 = 0.19 \pm 0.03,$$

$$I_3 = 0.17 \pm 0.03,$$

$$I_0 = 0.34 \pm 0.03. \quad (\text{C4})$$

About a third of the momentum is carried by gluons, and the number of λ quarks is slightly less than the number of \mathcal{P} quarks in the proton. This is a more plausible result.

It is interesting to perform a similar estimate under the assumption that the partons are "ordinary" particles with integer charges of isotopic spin 0, $\frac{1}{2}$, and 1. We divide them into four groups, $i = 1, \dots, 4$, according to what happens to their squared charge when the isotopic-spin component is reversed:

Group	What happens to e_i^2	Example
$i = 1$	$1 \rightarrow 0$	$p, \bar{\Xi}^-$
$i = 2$	$0 \rightarrow 1$	$n, \bar{\Xi}^0$
$i = 3$	$1 \rightarrow 1$	$\Sigma^+, \Omega, \bar{\Sigma}^+, \bar{\Omega}$
$i = 4$	$0 \rightarrow 0$	$\Lambda, \Sigma^0, \bar{\Lambda}, \bar{\Sigma}^0$

We must restrict ourselves to baryons and anti-baryons, since partons seem to have half-integer spins. Then category $i = 3, 4$ must be strange particles.

Using the same notation as before, we get

$$I_p = I_1 + I_3,$$

$$I_n = I_2 + I_3,$$

$$I_1 + I_2 + I_3 + I_4 + I_0 = 1,$$

and we obtain the following relation:

$$I_0 = 0.7 \pm 0.05 + I_3 - I_4. \quad (C5)$$

SU(3) symmetry requires that $I_3 > I_4$. It is seen, therefore, that $I_0 > 0.7$. Thus partons with integer charge would require that more than 70% of the momentum be carried by gluons. This is not a plausible result.

APPENDIX D

We follow closely the considerations of Bloom and Gilman.⁵ We determine the square of the form factor $G_s(Q^2)$ for the inelastic excitation of a level with the excitation energy expressed in units of $s = W^2$ as defined in (3.9). The average $\langle G_s^2(Q^2) \rangle_{av}$ over an interval ds containing several levels can be expressed in terms of the function W_2 ,

$$\langle G_s^2(Q^2) \rangle_{av} \rho(s) = W_2 \frac{d\nu}{ds} = \frac{F(x)}{2M\nu} = \frac{x F(x)}{Q^2},$$

where $\rho(s)$ is the level density and

$$\frac{x-1}{x} = \frac{s-M^2}{Q^2}.$$

We restrict ourselves to regions where $1-x \ll 1$, in which $F(x)$ can be expressed by (3.20), and we get (c is a constant)

$$\langle G_s^2(Q^2) \rangle_{av} \cong \frac{[\rho(s)]^{-1} c (s-M^2)^n}{Q^{2n+2}},$$

which shows that the inelastic form factor goes with $Q^{-(n+1)}$. This is valid as long as $(s-M^2) < (1-x^*)Q^2$, where x^* is the lower limit for the validity of (3.20). Bloom and Gilman maintain that the region $1-x \ll 1$ is dominated by the contribution of elastic scattering. This is certainly true if s is below the pion threshold, $M^2 < s \lesssim 1.5$. This region corresponds to $(1-x) \gtrsim 0.5/Q^2$. They predict that $F_n(x)/F_p(x) = (\mu_n/\mu_p)^2$ in that region. Our model cannot be applied to that region, as one can see from the following consideration: When $(1-x) \ll 1$, the quark which absorbs the light quantum has almost the full proton momentum, whereas the other "spectator quarks" have low momentum. After having absorbed the light quantum, the first quark is surrounded by the spectator quarks moving in the old direction. Since their momenta are low, they are able to join with the first quark by forming a combination of nucleon states of relatively low excitation, among which the ground state plays only a partial role. Hence, one concludes that our model can be applied only if averages are taken over several excited states, that is for $(1-x) > 0.5/Q^2$. We expect the ratio $F_n/F_p = \frac{2}{3}$ to be valid therefore in the region $0.5/Q^2 < (1-x) \ll 1$. We would expect that F_p is enhanced and F_n depressed for $(1-x) < 0.5/Q^2$ because of the coherent effect of the two quarks with parallel spin in the ground state of the nucleon.

*This work was supported in part through funds provided by the U. S. Atomic Energy Commission under Contract No. At(30-1)-2098.

†On leave of absence from Eotvos University, Budapest, Hungary.

¹R. P. Feynman, Phys. Rev. Letters **23**, 1415 (1969); in *High Energy Collisions*, Third International Conference, State University of New York, Stony Brook, 1969, edited by C. N. Yang, J. A. Cole, M. Good, R. Hwa, and J. Lee-Franzini (Gordon and Breach, New York, 1969).

²J. D. Bjorken and E. Paschos, Phys. Rev. **185**, 1975 (1969).

³S. D. Drell, D. J. Levy, and T. M. Yan, Phys. Rev. **187**, 2159 (1969); Phys. Rev. D **1**, 1035 (1970); **1**, 1617 (1970); S. D. Drell and T. M. Yan, *ibid.* **1**, 2402 (1970); Phys. Rev. Letters **24**, 181 (1970); Ann. Phys. (N. Y.) (to be published). In this section we follow Drell and Yan's normalization.

⁴For a summary of the experimental data, see the MIT-SLAC Report No. SLAC-PUB-796, 1970 (unpublished), presented at the Fifteenth International Conference on High Energy Physics, Kiev, U.S.S.R., 1970.

⁵E. D. Bloom and F. J. Gilman, Phys. Rev. Letters **25**, 1140 (1970).

- ⁶H. Harari, Phys. Rev. Letters **24**, 286 (1970).
⁷T. D. Lee, Columbia University report (unpublished).
⁸J. D. Bjorken, Phys. Rev. **148**, 1467 (1966).
⁹L. Galfi, P. Gnadig, J. Kuti, F. Niedermayer, and A. Patkos, Eotvos University report (unpublished), presented at the Fifteenth International Conference on High Energy Physics, Kiev, U.S.S.R., 1970. This paper contains further references.
¹⁰G. Domokos, S. Kovesi-Domokos, and E. Schonberg, Phys. Rev. D **3**, 1184 (1971); **3**, 1191 (1971).
¹¹R. P. Feynman, M. Kislinger, and F. Ravndal, Phys. Rev. D **3**, 2706 (1971).
¹²J. H. Christenson, G. S. Hicks, L. M. Lederman, P. J. Limon, B. G. Pope, and E. Zavattini, Phys. Rev. Letters **25**, 1523 (1970).
¹³J. D. Bjorken and E. Paschos, Phys. Rev. D **1**, 3151 (1970). This paper contains further references. G. Domokos, S. Kovesi-Domokos, and E. Schonberg, Johns Hopkins University report (unpublished).
¹⁴I. Budagov *et al.*, Phys. Letters **30B**, 364 (1969).
¹⁵Frascati report (unpublished), presented to the Fifteenth International Conference on High Energy Physics, Kiev, U.S.S.R., 1970.
¹⁶For a recent review, see G. Veneziano, in Proceedings at the International Conference on Duality and Symmetry in Hadron Physics, Tel Aviv, Israel, 1971 (unpublished).
¹⁷R. P. Feynman (private communication).

PHYSICAL REVIEW D

VOLUME 4, NUMBER 11

1 DECEMBER 1971

Dynamically Based Coupling Scheme for the Pomeranchukon

R. Carlitz*

*CERN, Geneva, Switzerland**and Institute for Advanced Study, Princeton, New Jersey 08540*

and

M. B. Green* and A. Zee

Institute for Advanced Study, Princeton, New Jersey 08540

(Received 8 July 1971)

We present a coupling scheme for the Pomeranchukon which relates its couplings to those of the f and f' trajectories. In this scheme the Pomeranchukon couplings factorize and transform as a combination of SU(3) singlet and octet in a prescribed ratio. This enables us to explain the observed deviation of the ratios of SU(3)-related total cross sections from their symmetry values and, qualitatively, the difference between πp and Kp diffraction slopes. A certain "universality principle" concerning the relative importance of Pomeranchukon exchange to f -trajectory exchange emerges in this scheme. This is tested with and supported by the available data on πp , pp , γp , and Kp total cross sections. The scheme accommodates quite naturally the observation of s -channel helicity conservation at high energies in πN scattering and ρ photoproduction. On the other hand, it does *not* predict s -channel helicity conservation in $\pi N \rightarrow A_1 N$. Indeed, we discuss the possibility that the observation of t -channel helicity conservation in this process may be understood on kinematical grounds. We stress that our coupling scheme is compatible with a large class of dynamical models which differ in their descriptions of the detailed nature of the Pomeranchukon. Thus, our successful confrontation with the available data must be credited to the indispensably essential assumptions that are shared by these different dynamical models.

I. INTRODUCTION

A fundamental fact of high-energy experiments is that elastic scattering and other processes which do not involve the exchange of quantum numbers are characterized by approximately constant cross sections at high energies. Such processes are known as diffraction scattering, as the shape of the differential cross section bears a distinct resemblance to that observed in classical diffraction scattering. They may be accommodated in the framework of Regge theory by introducing the

concept of the Pomeranchukon, which is by definition a singularity in the vicinity of $J=1$. The nature of this singularity is, however, unknown. Theorists have proposed moving poles, fixed poles, moving cuts, fixed cuts, double poles, and complex poles,¹ none of which can be decisively ruled out by the present data. The advent of larger machines and the consequent increased interest in multiparticle phenomena and inclusive experiments should eventually clarify the precise J -plane structure. Duality has further underscored the fact that the Pomeranchukon is most likely a qual-